

METABOLIC CHANGES IN OPTIC NERVE HEAD ASTROCYTES FOLLOWING GLAUCOMIC DEFORMATION

(70)

Thesis Advisor: Denise M. Inman

ABSTRACT

Glaucoma is an optic neuropathy that leads to irreversible blindness. The most common variant of glaucoma is typified by a chronic increase in intraocular pressure which causes a stretch injury to the optic nerve head. The predominant glial cell in this region is the optic nerve head astrocyte. As this region of the nerve is unmyelinated, the optic nerve head astrocyte provides axons their metabolic support, mainly by releasing lactate produced by astrocytic glycolysis. Our primary hypothesis is that stretching of the optic nerve head astrocytes changes their metabolic activity, thereby advancing glaucomic degeneration by hindering the metabolic support that the astrocytes provide to the axons in the optic nerve head. I will investigate the metabolic changes in optic nerve head astrocytes by subjecting them to stretch conditions similar to glaucoma. Using the FlexCell 6000T, I will stretch optic nerve head astrocytes and 1) collect the cells for proteomic analysis, and 2) passage cells into the Seahorse XFe 24 Analyzer to measure their oxygen consumption and extracellular acidification to determine the glycolytic and respiratory activity differences between control and stretched optic nerve head astrocytes. These approaches will yield data that establishes optic nerve head astrocyte metabolism and how it is altered by glaucoma-associated stretch injury.

METABOLIC CHANGES IN OPTIC NERVE HEAD ASTROCYTES  
FOLLOWING GLAUCOMIC DEFORMATION

A thesis submitted  
To Kent State University in partial  
Fulfillment of the requirements for the  
Degree of Master of Sciences

by

Nathaniel Pappenhagen

May 2021

© Copyright

All rights reserved

Thesis written by

Nathaniel Pappenhagen

B.S. Ohio Wesleyan University, 2015

M.S. Kent State University, 2021

Approved by

Dr. Denise Inman, Advisor

Dr. Ernest Freeman, Chair, Department of Biomedical Sciences

Dr. Mandy Munro-Stasiuk, Interim Dean, College of Arts and Sciences

**Table of Contents**

TABLE OF CONTENTS-----iv

LIST OF FIGURES-----v

ACKNOWLEDGEMENTS-----vi

INTRODUCTION-----1

METHODOLOGY-----11

RESULTS

    I.    Proteomics Results-----22

    II.   Metabolic Test Results-----25

DISCUSSION-----32

CONCLUSIONS-----43

REFERENCES-----49

## List of Figures

Figure 1: <i>Eye and Optic Nerve Anatomy</i> -----	3
Figure 2: <i>Schematic of the FlexCell 6000T Stretching the Cell Growth Membrane</i> -----	13
Figure 3: <i>Modified Glycolytic Stress Test Schematic</i> -----	17
Figure 4: <i>Mitochondrial Stress Test Schematic</i> -----	18
Figure 5: <i>Mitochondrial Fuel Dependency Test Schematic</i> -----	20
Figure 6: <i>Stretch Causes Increase in Glycolytic Activity in Optic Nerve Head Astrocytes</i> -----	26
Figure 7: <i>Stretch Alters Mitochondrial Respiration in Optic Nerve Head Astrocytes</i> -----	27
Figure 8: <i>Stretch Does Not Change Mitochondrial Fuel Dependency in Optic Nerve Head Astrocytes</i> -----	30
Figure 9: <i>Stretch Does Not Change Mitochondrial Fuel Flexibility in Optic Nerve Head Astrocytes</i> -----	31
Figure 10: <i>Metabolic Pathway Changes Schematic</i> -----	45
Figure 11: <i>Glutamine and <math>\alpha</math>-ketoglutarate Changes Schematic</i> -----	47

## Acknowledgements

I would be lying if I said I did this alone, and now I am able to rectify the solo authorship on my title page. I have had immeasurable help from many people along my path through this research, and the ultimate completion of this document. To begin with, I would like to thank Dr. Denise Inman for her help through this chapter of my life. Without meeting with her, I would not have come to KSU, moved to Texas, or potentially made it through graduate school. She helped me realize the depth of work to be done in science, and how I could do it without a PhD, something I was led to believe was necessary to pursue this career. I have learned countless things in her lab, from the mundanity of mouse colony management to what I want from my career and how I could make that happen. For all of that and more, I thank her.

Next, I would like to acknowledge the people I have worked alongside during my graduate school career. From the everyday camaraderie of Dr. Assraa Hassan Jassim to the talks of choir life with Kayla Trautman to the backyard party with Amelia Kline, I am grateful that my time in NEOMED was among friends. I am incredibly thankful for Charles “Chip” Kiehlbauch for being an example of the kind of life I can reach, and for talking with me about how to accomplish it. I have drawn strength and joy from all of you, even if I’ve been too reserved to express it properly.

I would also like to thank my committee members; Dr. Samuel Crish, Dr. Edgar Kooijman, and Dr. Abbot Clark. They have provided me with their time and help in making my research the best that it can be.

Finally, I would like to thank my friends and family outside of KSU/NEOMED/ENTERI. My friends Michelle, Eric, Robert, Blake and Kat have kept me grounded and reminded me that there’s more to life than work. My parents, Bob and Jill, have given me nothing but love and support to become the man I am today, and to find my way in life. In saving the best for last, I come to my fiancé, Ellie Carter. She has

given me the strength to take on new challenges, a safe place to rest, and a reminder that the best things in life are not done alone, but together.

## Introduction

### *What is Glaucoma?*

Glaucoma is an optic neuropathy that is the largest cause of irreversible blindness in the world (Weinreb et al., 2014). There are many varieties of glaucoma, the most common of which is primary open angle glaucoma (POAG). POAG is traditionally characterized by a chronic increase in intraocular pressure (IOP) caused by a decrease in aqueous humor outflow either through Schlemm's Canal in the trabecular meshwork of the eye (Figure 1A), or through the uvea/sclera. This increase in IOP puts pressure on the optic nerve head (ONH), causing strain. The ONH is the place where the axons of the retinal ganglion cells (RGCs) exit the eye and form the optic nerve. While POAG is the most common form of glaucoma, there are closed angle glaucomas, where the Schlemm's Canal is completely blocked, leading to an acute increase in IOP; secondary glaucomas that develop as side effects from medications and conditions; and even types of normal tension glaucoma characterized by no increase in IOP. In all of these glaucomas, the ON degenerates and leads to blindness as the retina gets disconnected from the brain.

The ONH is the initial site of degeneration in glaucoma. This has been demonstrated in human glaucomatic patients (Quigley et al., 1981), as well as rodent glaucoma models (Howell et al., 2007; Chidlow et al., 2011a). Elevated IOP causes optic cupping in human cases of glaucoma, a physical excavation of the ONH that signals degeneration of the RGC axons (Quigley and Green, 1978). This early axonal degeneration precedes the death of the RGC soma and is concurrent with dendritic arbor pruning in the retina (Berry et al., 2015; El-Danaf and Huberman, 2015). These early changes in glaucoma are accompanied by protein accumulation in the optic nerve head (Libby et al., 2005; Munemasa and Kitaoka, 2012; Crish et al., 2013). This cupping, loss of transport, and axonal loss is present in many *in vivo* models of glaucoma (Guo et al., 2005; Chidlow et al., 2011b; Wilson et al., 2016; Maddineni et al.,

2020). These changes and damage point to the optic nerve head as an important region for understanding glaucoma.

### *What is the Optic Nerve Head?*

The ON is part of the central nervous system, and is made up of RGC axons and glial cells. The regions of the optic nerve include the chiasm, the anterior nerve, and the ONH. The ONH is an unmyelinated portion of the nerve immediately posterior to the eye where the RGC axons pass through the lamina cribrosa, a network of collagen and elastin that is thinner and less dense than the sclera, the tough tissue that forms the outer layer of the eye (Figure 1B). The lamina cribrosa cells are accompanied by astrocytes, which support the axons in the absence of myelin in the ONH. The ONH is a place of great mechanical stress in glaucoma. The distension of the eye through the lamina cribrosa causes the optic disc and the ONH to press back through the lamina cribrosa, leading to a chronic 9% stretch (Girard et al., 2016). This cupping accompanies RGC loss, axonal transport loss, and visual field loss. Optic nerve head astrocytes (ONHAs) react to this stretch in glaucoma, which in turn affects their neighboring axons.

The astrocytes in the ONH enter a state of reactivity and hypertrophy that impacts the health of the RGCs they are supposed to be supporting. Reactive astrocytes negatively impact neurons through the generation of pro-inflammatory molecules in addition to changes in metabolic support. These can lead to impacted axonal transport, mismanaged metabolism, and degeneration (Chung et al., 2009; Vohra et al., 2013; Iglesias et al., 2017). Our lab has shown that altering the metabolic profile of retina and ON in glaucomic animals has an inhibitory effect on neuroinflammation through upregulation of hydroxycarboxylic acid receptor 1 (HCAR1) and lowered AMP-kinase (AMPK) activation, a receptor that responds to lactate among other molecules and a metabolic monitoring protein, respectively. Resolving inflammation is one way that we can lower the harm of glaucoma.

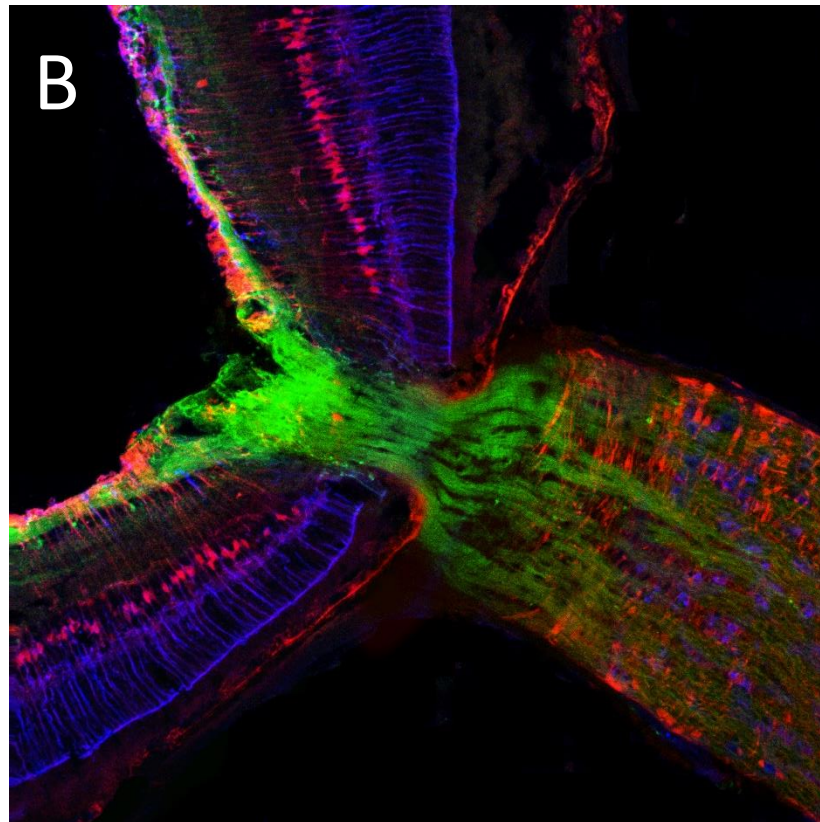
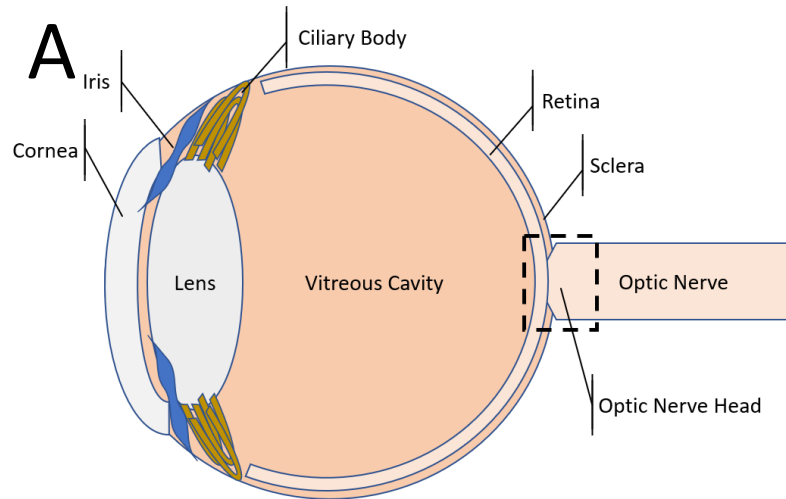


**Figure 1** Eye and Optic Nerve Head Anatomy. A: Stylized image of the anatomy of the human eye. The sclera is the tough white outer covering of the eye. The ciliary body is the site of aqueous humor production. Lens zonules that emerge from the ciliary epithelium hold the lens in place and contract to allow accommodation. The iris sits in front of the lens, forming the pupil which controls the amount of light that gets into the eye. B: Cross section of a mouse central retina and proximal optic nerve showing the optic nerve head (ONH). Aldehyde 111 (red) is an astrocyte-specific marker, as is glial fibrillary acidic protein (blue); cholera toxin B (green) labels axons of the retinal ganglion cells. The ONH is where the retinal ganglion cell axons (green) converge, exiting the eye; it extends as far as the beginning of optic nerve myelination.

Hypertrophy of the astrocytic processes is another change that accompanies astrocyte activation in glaucoma. In non-glaucomatic tissue, ONH astrocytes have processes that span the width of the ONH (Sun et al., 2010; Dai et al., 2012). These processes allow astrocytes to support many axons at a time, and organize them into bundles that will be maintained through the white matter tract of the ON (Minckler, 1980). When the IOP elevation of glaucoma begins, these processes retract to the cell body and no longer reach across the nerve. Another element of the reorganization of the ONH is the transformation of the extracellular matrix, effected by transforming growth factor- $\beta$ 2 release from astrocytes and lamina cribrosa cells. Transforming growth factor  $\beta$ 2 (TGF- $\beta$ 2) is a harmful cytokine that is released in glaucomatic eyes (Fuchshofer, 2011; Zode et al., 2011; Wordinger et al., 2014). It increases the expression of extracellular matrix (ECM) proteins such as collagen I, collagen IV, and fibronectin in primary ONHA cultures (Zode et al., 2011). Increases in these structural proteins could have detrimental effects on the flexibility of the ONH, and in turn subject the ONH to more strain than in tissues without increased ECM protein expression (Zhang et al., 2015). Decreasing the effect of TGF- $\beta$ 2 on the ECM by the use of its inhibitor bone morphogenic protein 4 reduced the production of fibronectin, collagen I, collagen IV, elastin and plasminogen activator inhibitor-1 in cultured ONHAs (Zode et al., 2009). The hypertrophic astrocyte changes along with the changes in the ECM proteins in the glaucomatic ONH could have myriad consequences, ranging from loss of contact with cells they are meant to support to a lack of physical support and organization that the astrocytes are responsible for in the nerve head.

#### *What Metabolic Changes Accompany Glaucoma?*

Glaucoma is accompanied by metabolic changes in the optic nerve and retina. The glaucomatic nerve changes the expression of its metabolic transporters, oxygen utilization, and cellular respiration.

These changes play an integral role in glaucomic degeneration, and alleviating these stressors proves beneficial to slowing the progression of degeneration.

We have demonstrated changes in metabolic transporter profiles in glaucomic tissues (Harun-Or-Rashid et al., 2018). Glucose transporter 1 (GLUT1), the primary glucose transporter found on epithelial cells and astrocytes (Morgello et al., 1995), is decreased in ON in a chronic mouse model of glaucoma as measured by capillary electrophoresis protein analysis and immunofluorescence (Harun-Or-Rashid et al., 2018). Additionally, monocarboxylate transporter (MCT) 1, MCT2 and MCT4 are decreased in glaucomic ON. These proteins are transporters of the monocarboxylate molecules, including lactate, pyruvate, and ketone bodies (Halestrap, 2012). These downregulations in transporter proteins suggest metabolic shifts accompany glaucomic degeneration as the glial cells and RGCs form a metabolic unit of cells working together to maintain the metabolic activity of each other. This co-dependency is described by the lactate shuttle hypothesis. This hypothesis proposes that glial glycolysis produces lactate to be exported to neighboring neurons for conversion to pyruvate and as fuel for mitochondrial respiration (Pellerin et al., 1998; Volkenhoff et al., 2015; Saab et al., 2016; Muraleedharan et al., 2020). Glucose entry to this metabolic unit would be decreased by the loss of GLUT1, and the lactate shuttle activity would be decreased as well. This would ultimately limit the energy availability in the RGC axons in the ON, which is detrimental for the health of the glaucomic nerve.

Altering metabolic activity in mouse models of glaucoma has had protective effects for RGCs. We have increased metabolic activity in glaucomic animals by using a ketogenic diet to increase mitochondrial activity and by using an adeno-associated virus to increase monocarboxylate transporter-2 expression, thereby increasing metabolic substrate availability in glaucomic tissues (Harun-Or-Rashid et al., 2018, 2020a). Other research has shown that glaucomic retina has lower nicotinamide adenine dinucleotide (NAD<sup>+</sup>) concentration compared to control animals, and that its restoration with administration of vitamin B<sub>3</sub> protects RGCs in glaucomic animals (Williams et al., 2017). NAD<sup>+</sup> is

important to the metabolic health of the RGCs as an electron carrying molecule in the citric acid cycle and glycolysis. Its loss occurs before significant ON degeneration has occurred, and treatment of glaucoma patients with a NAD<sup>+</sup> supplement increased inner retina function (Hui et al., 2020)

ONs isolated from mice with elevated intraocular pressure (IOP) have been shown to have lower ATP concentrations than age matched ON with normal IOP (Baltan et al., 2010). This correlates with a loss of compound axon potential (CAP) propagation along the ON observed in age-matched DBA/2J (D2) mice. These mice possess two genetic mutations that cause an iris pigment dispersion disease that leads to a secondary glaucoma, with chronically raised IOP and consequences to the RGCs that resemble primary open angle glaucoma (Anderson et al., 2002; Libby et al., 2005; Saleh et al., 2007). The loss of ATP production and ON function is linked to IOP elevation in glaucoma models, further implying a link between glaucoma and metabolic dysregulation. The decrease in CAP propagation and ATP production, as well as the lowered concentrations of GLUTs and MCTs that compromise movement of metabolic substrates between cells or from the bloodstream (as discussed above (Harun-Or-Rashid and Inman, 2018)), indicates there is more to glaucomic degeneration than just physical damage caused by elevated IOP.

Other metabolic challenges in glaucomic tissue include a reduction in blood flow to the retina and ON (Flammer et al., 2002), an increase in autophagy (Coughlin et al., 2015), and increase of inflammation (Harun-Or-Rashid and Inman, 2018). While reductions in blood flow can be caused by elevated IOP impacting the eye's vasculature, these other changes are not. Early interruptions to blood flow and axonal transportation cascade into larger problems with metabolic dysregulation, such as the increased autophagy, inflammation, and decreased metabolic transporter expression (Buckingham et al., 2008; Coughlin et al., 2015; Harun-Or-Rashid et al., 2018).

Our lab has shown that glaucomic ON has a higher glycolytic rate and impaired glycolytic responsiveness than control ON by measuring the extracellular acidification rate (ECAR) as well as measuring glycolytic increase after inhibiting mitochondrial ATP production in ex vivo DBA/2J (D2) and control DBA/2J<sup>GPNMB<sup>+</sup></sup> (D2G) ON (Jassim et al., 2019). ONs were isolated from a time course of D2 mice, and placed in a Seahorse instrument to measure oxygen consumption rate (OCR) and extracellular acidification rate (ECAR). Ten-month-old D2 ON had higher baseline ECAR and lower maximal ECAR than 10-month-old D2G ON. Properly controlled ECAR experiments can be used to measure the glycolytic activity of cells and tissues, as glycolysis ends with the export of lactate and a proton from the cell. Additionally, 10-month-old D2G ON showed a higher ratio for ATP production from OCR compared to ECAR. This suggests that in the control ON, the tissue is undergoing more cellular respiration than the glaucomatous ON.

Our lab has observed that addressing the metabolic inadequacies in the glaucomic ON is protective against the degeneration of the RGCs. We first tested the hypothesis that RGC survival would result through a selective diet to promote mitochondrial respiration over glycolysis, the ketogenic diet (KD) (Harun-Or-Rashid et al., 2018). This diet is 89.5% fat, which is metabolized by the liver into fatty acids and  $\beta$ -hydroxybutyrate, a ketone body that can feed into the tricarboxylic acid cycle (TCA), promoting mitochondrial respiration. The diet prevented RGC degeneration, increased MCT2 protein, and improved succinate dehydrogenase (SDH) and cytochrome-c oxidase (COX) activities. SDH and COX are both enzymes used for mitochondrial respiration and their increase following treatment with the ketogenic diet suggests that the treated nerve became more mitochondrially active (Harun-Or-Rashid et al., 2020b).

Overexpressing MCT2, the MCT responsible for allowing lactate into neurons (which is downregulated in glaucoma), rescued RGC and axon loss in two models of glaucoma (Harun-Or-Rashid et al., 2020b). The neurons overexpressing MCT2 had an increased ability to pick up lactate produced in

glial cells, then use it for mitochondrial respiration by converting it into pyruvate and fueling the TCA cycle. The increase in COX and SDH activity in the glaucomic tissue with MCT2 overexpression paired with an overall decrease in hexokinase 1 (HK1) activity suggested a shift in the MCT2 overexpression nerves towards mitochondrial respiration and away from glycolysis.

#### *What Happens Metabolically in Reactive Astrocytes?*

The metabolism of astrocytes changes when they are activated. Astrocytes that have been made reactive *in vitro* using amyloid- $\beta$  as a model of Alzheimer's Disease (AD) increase their glycolytic activity as well as the products of glycolysis such as lactate export, TCA cycle activity, and pentose phosphate pathway activity (Allaman et al., 2010). Under hypoxic conditions, another method to generate reactive astrocytes *in vitro*, reactive astrocytes also showed increased glycolytic activity as measured by the lactate production to glucose consumption ratio (Amaral et al., 2010). Interestingly, further investigation into *in vivo* models of neurodegeneration typically show altered glycolytic metabolism. In AD brains, there are lowered expressions of glucose transporters, and hypometabolism in regions of the brain experiencing degeneration (Costantini et al., 2008; Steele and Robinson, 2012; Tang, 2020). Parkinson's Disease patients have lowered glycolytic rates in brain regions that are degenerating in the disease, and a drug (terazosin) is in clinical trials to prevent Parkinson's Disease-associated degeneration by increasing glycolysis and downstream metabolic processes (Huang et al., 2008; Foltynie, 2019). Glaucomic ONs have been shown to have higher baseline glycolytic activity, but a lowered ability to increase glycolysis when challenged (Jassim et al., 2019). Even in aging, glycolytic metabolism is altered as insulin, neurotrophic factors and thyroid hormones change in the brain and affect glycogen storage, glycolysis and lipid synthesis (Clarke et al., 2018; Morita et al., 2019). Reactive astrocytes in myriad neurodegenerative conditions face challenges in their normal glycolytic activity and neuronal support, making their metabolic activity a potentially therapeutic target in glaucoma.

### *Why is this Important?*

The ONH is the locus of degeneration in glaucoma. The changes that occur here at the beginning of the neurodegenerative disease are first felt here, and understanding that helps open up new treatments for glaucoma. Metabolic changes in one part of the metabolic unit impact other parts of the unit. If reactive astrocytes in the ONH are more glycolytic, then they could be providing more metabolic support to the neurons. Other implications of a potential increase in glycolytic activity could be extracellular acidification as lactate export from the cell requires a proton to pass as well. Increases in fatty acid oxidation pathways, as is seen in reactive astrocytes in other conditions, could also prove potentially challenging to the ONH because it experiences hypoxia in glaucoma (Tezel and Wax, 2004; Chidlow et al., 2017; Jassim and Inman, 2019; Jassim et al., 2021). Increased glycolysis for the export of lactate while relying on fatty acid oxidation for increased ATP production could be problematic in a hypoxic environment, especially as fatty acid oxidation uses more oxygen to oxidize fatty acids to an appropriate length before they can be used in mitochondria for ATP synthesis. The expectation in a hypoxic environment is a transition to glycolysis because glycolysis does not require oxygen to generate ATP, and hypoxia upregulates the transcription factor HIF-1 $\alpha$  that promotes glycolytic enzymes (Lum et al., 2007; Nagao et al., 2019). However, we must square the likely increases in glycolysis with our observations of decreased glycolytically regulatory proteins such as glucose transporter 1 and monocarboxylate transporter 1 and 4 (Harun-Or-Rashid et al., 2018; Tanner et al., 2018). It might be that glaucomic ONHAs utilize glycolysis to a lesser degree than control ONHAs because they face troubles importing glucose and exporting lactate, impairing not only the ONHA's metabolism, but also the neurons that rely on lactate import for the firing of action potentials and normal metabolic activity (Volkenhoff et al., 2015; Suplie et al., 2017). On the other hand, ONHAs may be able to increase their glycolysis in the midst of overall decreases in glucose transporters because there are fewer overall cells in the ONH during glaucoma-associated degeneration. Astrocytes carry glycogen stores that may also

temporarily meet glycolytic needs in the absence of glucose transporters. Lastly, astrocytes depend on each other in times of stress, using their gap junctions to transport glucose among themselves (Cooper et al., 2020). These experiments were designed to shed light on the many unknowns associated with glaucoma-associated metabolic change in the ONH.

### *What is our Hypothesis?*

We are interested in observing the metabolic changes that occur in glaucomic ONHAs. We believe that this will provide insight into the metabolic environment of the ONH in glaucoma, and potentially the detrimental changes that occur therein. The long-term goals of the lab are to understand the metabolic changes in the ONHAs in glaucoma, specifically the glycolytic and mitochondrial activity in these cells to identify therapeutic targets for glaucoma related to astrocyte-neuron metabolic interaction. My central hypothesis is that optic nerve head astrocytes acted upon by glaucoma-associated stressors will change their expression of metabolically active proteins and their metabolic activity. I will test this hypothesis using primary ONHAs deformed in a manner similar to glaucoma as an *in vitro* model of the conditions in the ONH. I will use proteomic analysis of these stretched astrocytes, and bioenergetic analysis of stretched and control astrocytes, measuring oxygen consumption and extracellular acidification to determine the metabolic changes caused by mechanical stretch.

## Methods

### Primary Cell Isolation Methods:

#### *Primary Cortical Astrocyte Isolation:*

Primary cortical astrocytes were isolated from P0-1 mouse pups, using slightly modified methods from the Johnson Lab (Lee et al., 2003). P0-1 mice were sacrificed by decapitation. A midline incision from base of skull to the nose, through the skin, then through the skull revealed the brain, which was removed with forceps and placed on a sterile petri dish for dissection. The hind brain and midbrain were removed with razors and forceps before the remaining cortex was placed in 5 mL of ice-cold digestion solution made of 0.025% trypsin and 0.02% ethylenediaminetetraacetic acid (EDTA) in sterile phosphate buffered saline (PBS). Once all pups from the litter were sacrificed (typically between 5 and 8), the cortices in digestion solution were placed in a 37°C water bath to digest for 30 minutes, being gently agitated every 10 minutes. After digestion, the cortices were spun down at 1000 RPM, then the digestion solution was removed and replaced with 5mL astrocyte growth media. The cortices were then triturated into a single cell suspension using serological pipettes. The single cell suspension was then plated at a density of 3 brains per T-75 and allowed to grow for 4-5 days.

Primary cortical astrocytes were cultured in astrocyte growth media made up of DMEM with 4.5 mg/mL, 2 mM glutamine, 1 mM NaPyruvate, 1x Penicillin/Streptomycin and 1:10 heat-inactivated fetal bovine serum (HIFBS). After being allowed to settle and grow, the cells were shaken at 200 RPM for 30 minutes to dislodge non-astrocytic cells before being passed into experimental or growth culture plates. Cells were passed after reaching confluence. Media was removed, the cells were washed once with sterile PBS, and then incubated with TrypLE (Gibco) for 3 minutes at 37°C. An equal amount of growth media was added to the TrypLE and cells to stop the digestion, and the mixture was then centrifuged for one minute at 1000 RPM to pellet the cells. Cells were then re-suspended in growth media and counted.

Cells (150,000 per well) were added to 2 mL of growth media in FlexCell 6000T plates coated with 200 µg/mL type 1 collagen to grow to confluence before the stretch experiments.

*Primary Optic Nerve Head Astrocyte Isolation:*

Primary optic nerve head astrocytes (ONHAs) were isolated from P6-7 rat pups using methods based on the works of the Kaja lab (Kaja et al., 2015). P6-7 rat pups were sacrificed by decapitation, their eyelids were cut open with a scalpel, and their eyes and ON cut out with iridectomy scissors. Removed eyes were placed in petri dishes, and the optic nerve head was removed with forceps and iridectomy scissors. Each optic nerve head explant was placed into one well of a 24-well plate, and allowed to dry out slightly to adhere to the plate. After 2 minutes, 1 mL of astrocyte growth media (DMEM with 4.5 mg/mL, 2 mM glutamine, 1 mM NaPyruvate, 1x Penicillin/Streptomycin and 1:10 HIFBS) was added to the explants. Astrocytes were then allowed to grow out from the explants for 5-7 days before they were passed similarly to the primary cortical astrocytes, with additional filtration through a sterile 100 µm filter before centrifugation and TrypLE removal and plating.

Primary ONHAs were placed into T-75s to grow after moving them from the 24 well plates, grown to confluence, and shaken at 200 RPM for 30 minutes at room temperature to remove any non-astrocytic cells. ONHAs (150,000 per well) were then seeded on 6-well FlexCell culture plates coated with 200 µg/mL genetic type 1 collagen, for the stretch experiments.

*FlexCell 6000T Stretch Experiments:*

Primary cells were stretched in a manner similar to that experienced in the optic nerve head (ONH) in glaucoma (Downs et al., 2008; Girard et al., 2016). The FlexCell 6000T uses vacuum to pull the membrane on which the cells are seeded over a plastic post, thus stretching them biaxially (Figure 2). We used a 12% sinusoidal stretch protocol with a 1 Hz frequency for 24 hours to imitate glaucomic stretch in the cultured cortical astrocytes and ONHAs, and to be in line with other research done on

mechanical stretch in primary ONH cells and astrocytes (Rogers et al., 2012a, 2012b; Albalawi et al., 2017).

Control primary cells were grown on 6-well FlexCell plates coated with 200  $\mu\text{g}/\text{mL}$  type 1 collagen until confluency before being collected for the proteomics or Seahorse experiments.

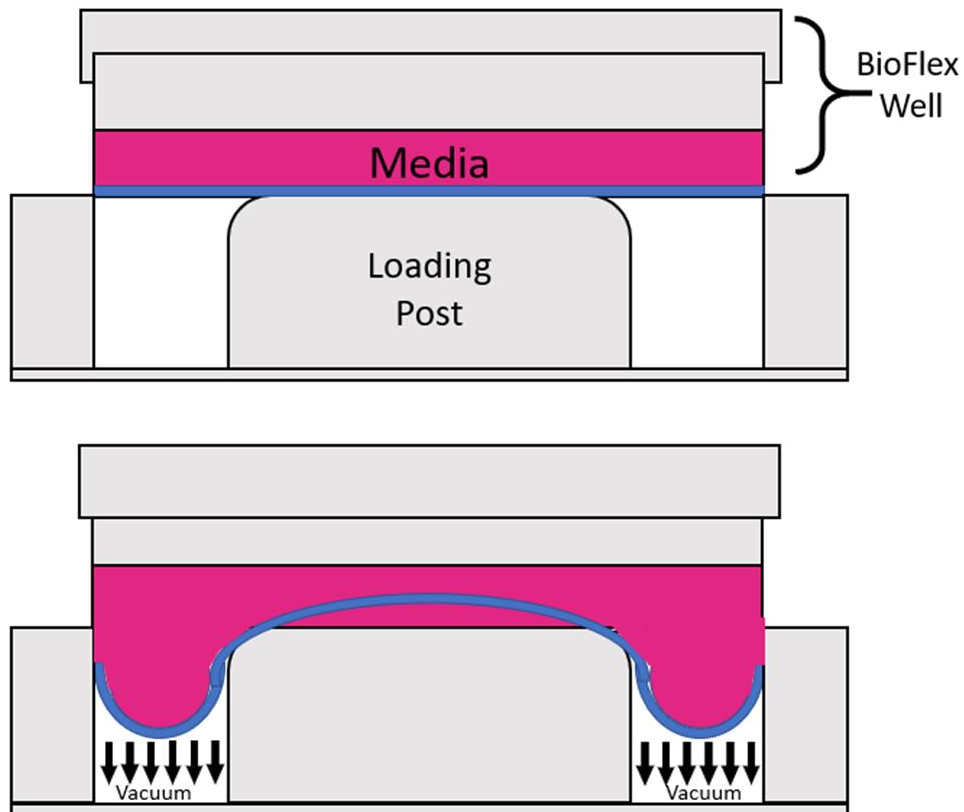


**Figure 2:** Schematic of the FlexCell 6000T Stretching the Cell Growth Membrane. Cells are grown to confluency in the BioFlex wells that have been coated with collagen-1, and the plates are then placed on the baseplate in a 37 °C incubator. A: Each well in the plate is placed over a lubricated loading post. B: When the stretch experiments begin, the FlexCell 6000T creates a vacuum under the BioFlex plates, which pulls the membrane against the post, and stretches the cells biaxially as the membrane is pulled from all around the post.

Proteomic Experiments:

*Isolation and Purification of Protein for Mass Spectrometry:*

Following control or FlexCell 6000T stretch experiments, cells were collected and processed for mass spectrometry. Deformed cortical astrocytes or ONHAs were pulled from the plates using a 3-minute incubation with TrypLE at 37°C, stopped by an equal volume of growth media, and pelleted by

centrifugation at 1,000 RPM for 1 minute. The cell pellet was then resuspended in 1 mL of astrocyte growth media for counting using the Countess (Life Technologies), and then pelleted again at the same centrifugation speed and time.

The cell pellets were then purified using the ThermoScientific Easy Pep Mass Spectrometry Sample Prep Kit for purification of mass spectrometry samples. In brief, the pellet was resuspended in lysis buffer and a universal nuclease at a volume of 100  $\mu\text{L}/1 \times 10^6$  cells, digested, then filtered through collection columns, leaving purified peptides. The peptides were then dried in a vacuum centrifuge before being held at  $-70^\circ\text{C}$  until mass spectrometry.

*Mass Spectrometry Measurement:*

Peptides were analyzed using a hybrid ion trap-Orbitrap tandem mass spectrometer (LTQ Velos Orbitrap Pro) coupled to an EASY nLC-1000 nanoflow liquid chromatography system fitted with a 15x75  $\mu\text{m}$  i.d. EasySpray column packed with 3  $\mu\text{m}$  PepMap C18 particles (Thermo Fisher Scientific, San Jose, CAA, United States). Experimental protocols were the same as previously run in other retinal proteomic experiments (Prokai et al., 2020). In brief, samples were reconstituted in 100  $\mu\text{L}$  of water with 5% acetonitrile acid and 0.1% formic acid and were eluted at 300 nL/min using a gradient for the mass spectrometry experiment. Full scan mass-spectra were obtained at 60,000 resolution using the Orbitrap, and up to 250 MS-dependent tandem mass spectra were obtained in the iso-trap for full spectrum.

*Database Generation and Statistical Analysis:*

Full spectra were searched against the UniProt database (species: *Rattus norvegicus*, 29938 entries) using the Mascot search engine (version 2.6.2; Matrix Science, Boston, MA, USA) run from Proteome Discoverer (version 2.3; Thermo Fisher Scientific. Parent ion mass tolerance was set to 25 PPM and fragment ion mass tolerance was 0.80 Da with only one missed cleavage for the search parameters. Scaffold Software (version 4.9.0, Proteome Software Inc.; Portland, OR, USA) was used to validate the results with Peptide Prophet and Protein Prophet algorithms. The spectral counting

provided by the Scaffold software and a  $p$  value of less than 0.05 was used to determine statistical significance, while a two-fold change was used to determine biological significance.

#### *CellTak Adhesion to Seahorse Plates*

CellTak-coated Seahorse plates were prepared prior to the addition of the ONHAs by incubating the plates with 22.4  $\mu\text{g}/\text{mL}$  CellTak for 20 minutes before washing it off twice with sterile  $\text{DDH}_2\text{O}$ . Once the ONHAs were finished in the FlexCell 6000T, they were removed with TrypLE as previously described, resuspended in 1 mL of the appropriate Seahorse assay media (plain DMEM with 2 mM glutamine for the glycolytic stress test, and plain DMEM with 2mM Glutamine, 1 mM NaPyruvate, and 1 mM glucose for mitochondrial stress test, mitochondrial fuel dependency test, and mitochondrial fuel flexibility test), and seeded in 100  $\mu\text{L}$  of the appropriate assay media (plain DMEM with 2 mM glutamine for glycolytic rate assay, and plain DMEM with 2mM glutamine, 1 mM NaPyruvate, and 1mM glucose for the other assays) on the CellTak-coated Seahorse plates. Plain DMEM without phenol-red with 2 mM glutamine was used as the assay media for the glycolytic stress test, and plain DMEM without phenol-red with 1 mM glucose 1 mM Na-pyruvate and 2 mM glutamine was used as the assay media for the mitochondrial stress test, mitochondrial fuel dependency test and mitochondrial fuel flexibility test. The plates with cells were spun at 200g for 1 minute with no braking, and incubated at 37°C in an incubator without  $\text{CO}_2$  for 25 minutes before the final 400  $\mu\text{L}$  of Seahorse assay media was added to each well. The plates were then ready for the Seahorse experiment.

#### Seahorse XFe 24 Analyzer

The Seahorse XFe Analyzer is an instrument that measures oxygen and pH in cells or tissue using fiber optic sensors. Oxygen consumption rate as determined for the cells allows the user to estimate mitochondrial respiration while released protons can be used to estimate lactate release, a measure of glycolytic activity. Injection ports for each culture well allows the user to add drugs to challenge cellular metabolic processes. We used the glycolytic rate assay, the mitochondrial fuel flex test, and the

mitochondrial stress test protocols to measure the metabolic changes in ONHAs following glaucoma-like stretch.

*Modified Glycolytic Stress Test:*

In the modified glycolytic stress test, cells start in DMEM media with 2 mM glutamine (no glucose or sodium pyruvate). This deprives the cells of glucose for glycolysis to allow for a baseline measurement of the extracellular acidification rate (ECAR) before the addition of glucose with the first injection. Once glucose is added, ECAR often increases; the difference between baseline and post-glucose injection is the ECAR associated with glycolysis. With the injection of 0.5  $\mu$ M rotenone and 0.5  $\mu$ M antimycin-a, Complex I and Complex III inhibitors, respectively, mitochondrial respiration in the cells ceases. This results in an increase in glycolytic activity and ECAR due to the cells responding to the loss of mitochondrial adenosine triphosphate (ATP) production. Finally, addition of 50 mM 2-deoxyglucose (2-DG), a non-hydrolyzable form of glucose added in excess, competitively inhibits hexokinase, thereby stopping glycolysis, and restoring cells to their baseline ECAR. The maximal glycolytic rate is defined as the maximal ECAR minus the baseline ECAR, and the glycolytic reserve is the maximal ECAR minus the glycolytic ECAR.

Cells were removed following the glycolytic rate assay and fixed for 15 minutes at 37°C with 2% formaldehyde. They were then labeled with 1:1000 4',6-diamidino-2-phenylindole (DAPI) in Tris-buffered saline (TBS) for 10 minutes, then rinsed with PBS with 0.1% azide for storage until the cells were counted for normalization. Figure 3 shows an example of the compound additions for the modified glycolytic stress test, and the math used to determine the glycolytic ECAR, maximal ECAR, and the

difference between maximum ECAR and glycolytic ECAR.

## Modified Glycolytic Stress Test

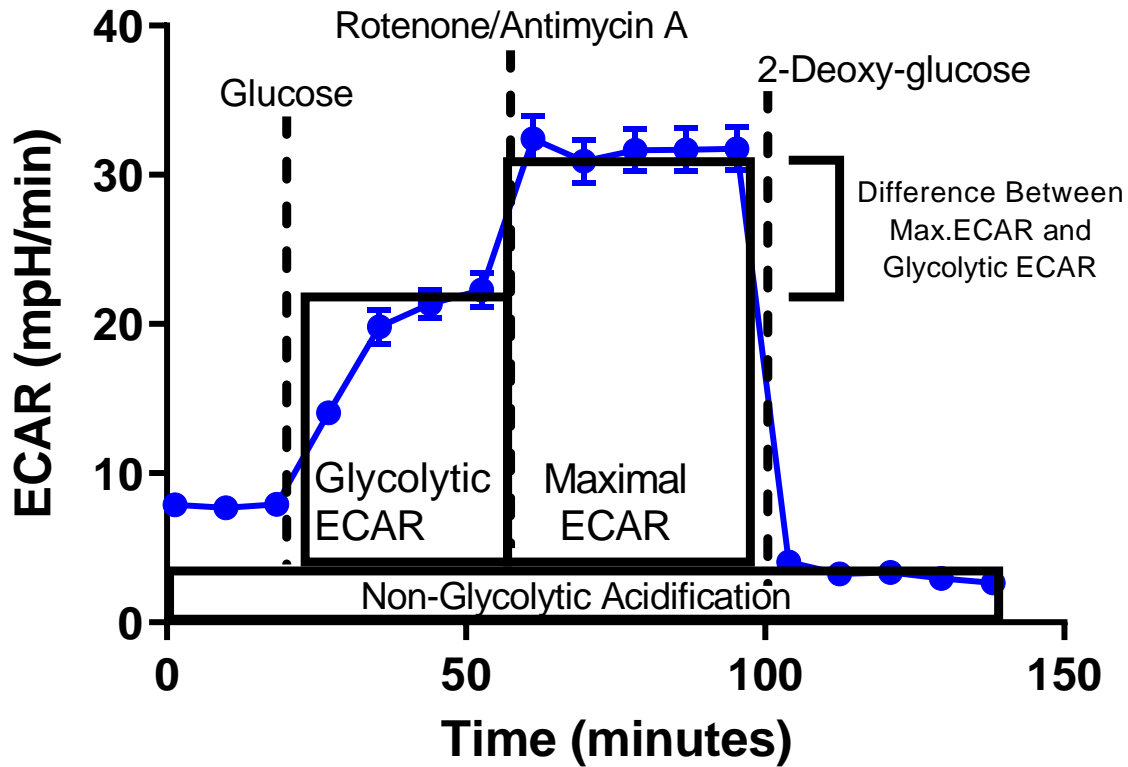


**Figure 3: Modified Glycolytic Stress Test Schematic.** The graph shows the compound addition times, and values used to estimate glycolytic activity in stretched and control ONHAs. Glycolytic ECAR represents the ECAR following glucose addition to the wells, with the non-glycolytic acidification subtracted. Maximal ECAR was the final ECAR reading following rotenone/antimycin-a addition, and the difference between the maximal ECAR and glycolytic ECAR was used to estimate glycolytic spare capacity.

## Mitochondrial Stress Test

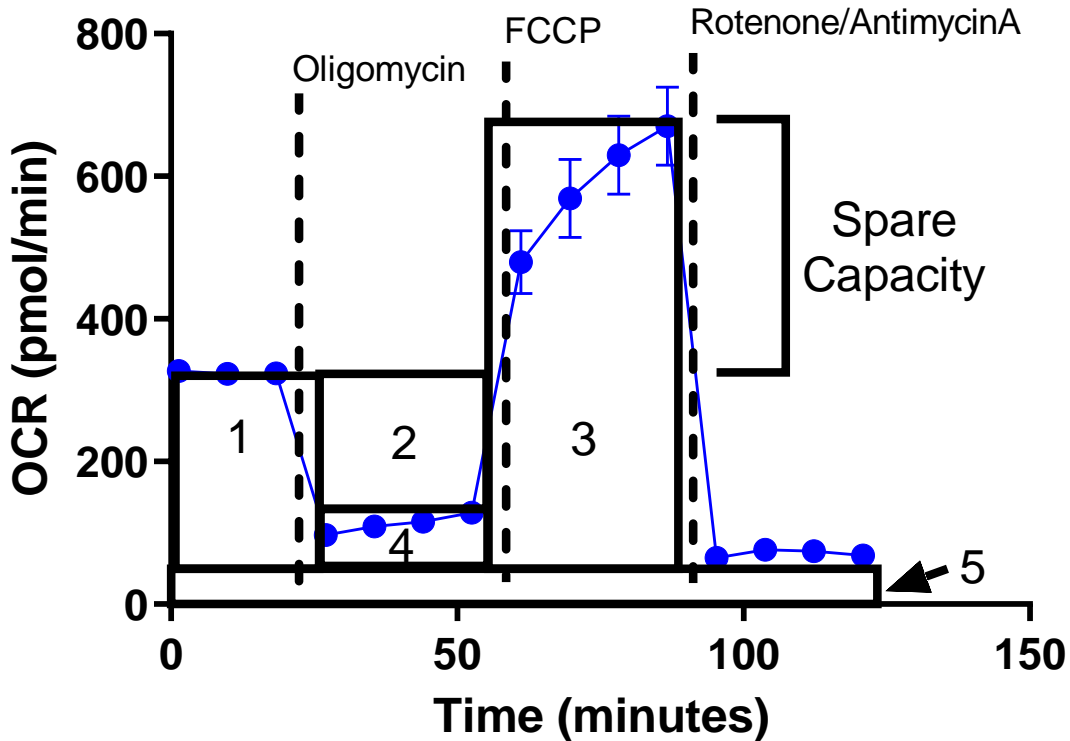


**Figure 4: Mitochondrial Stress Test Schematic.** The graph at right shows the compound additions and calculations within the mitochondrial stress test. 1: Baseline OCR was the baseline OCR with the non-mitochondrial OCR (5) subtracted. 2: ATP-linked OCR was the baseline OCR (1) with the non-ATP-linked OCR (4) subtracted. 3: Maximal OCR was the final measurement taken following the addition of FCCP with the non-mitochondrial respiration (5) subtracted. Spare capacity was defined as the maximal OCR (3) with the baseline OCR (1) subtracted from it.

### Mitochondrial Stress Test:

The mitochondrial stress test measures oxygen consumption rate (OCR) in response to serial injection of an inhibitor of ATP synthase (oligomycin-a), a protonophore (Trifluoromethoxy carbonylcyanide phenylhydrazone, FCCP), and electron transport chain complex I and III (rotenone and antimycin-a). The base media is DMEM with 1 mM glucose, 1 mM sodium Pyruvate, and 2 mM glutamine. After baseline OCR measures, an injection of oligomycin (1 mM) typically halts mitochondrial respiration-associated ATP production and the OCR falls; the difference between baseline OCR and OCR

during oligomycin-a exposure is considered the oxygen consumption attributable to ATP production. The protonophore FCCP (2 mM), by uncoupling the mitochondrial membrane potential from ATP production, leads to an increase in oxygen consumption (maximal respiration) as the electron transport chain (ETC) tries to maintain the proton gradient. Finally, rotenone and antimycin-a (0.5  $\mu$ M each) inhibit Complexes I and III, respectively, thereby completely shutting down respiration-associated OCR.

Following analysis using the Seahorse Analyzer, cells were fixed and labeled with DAPI as previously described. Figure 4 is a schematic of the mitochondrial stress test showing compound additions and the math used to determine the mitochondrial response to various stressors.

#### *Mitochondrial Fuel Dependency Test:*

The mitochondrial fuel dependency test was used to test the reliance of the mitochondria on three of the most common mitochondrial substrates; pyruvate, glutamine, and long chain fatty acids (LCFAs). The assay is run in triplicate on a single plate, with 6-7 wells dedicated to each fuel dependency. The assay uses 2-cyano-3-(1-phenyl-1H-indol-3-yl)-2-propenoic acid (UK5099) to inhibit pyruvate transport to the mitochondria, bis-2-(5-phenylacetamido-1,3,4-thiadiazol-2-yl) ethyl sulfide (BPTES) to inhibit glutamine transport into the mitochondria, and etomoxir to inhibit LCFA transport into the mitochondria. To determine the mitochondrial dependency on each fuel source, the compound inhibiting the substrate is added to the well, changes in OCR are measured, then the other two compounds are added, and the difference is measured. For example: to measure pyruvate dependence, first the baseline OCR is measured in the experimental wells, then UK5099 is added, more OCR measurements are taken, finally BPTES and etomoxir are added and the OCR is measured again. The difference in the UK5099 OCR and the baseline OCR compared to the difference in the OCR with all three compounds present and the baseline. Figure 5 is a schematic for the mitochondrial fuel dependency test, showing compound additions and calculations needed for the assay.

## Pyruvate Dependency

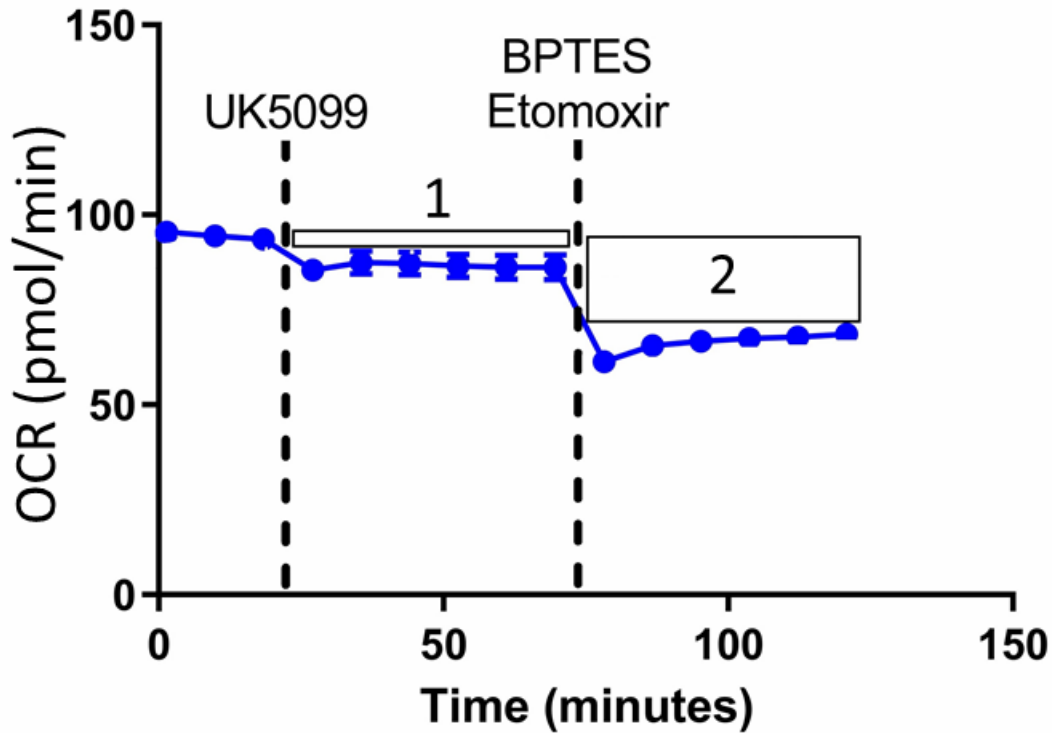


**Figure 5: Mitochondrial Fuel Dependency Test Schematic.** Shown here is an example run for the mitochondrial fuel dependency test, specifically for pyruvate dependency. Baseline OCR measurements are taken, followed by addition of one of the inhibitors of either the mitochondrial pyruvate carrier (UK5099), the inhibitor of long-chain fatty acid translocation (Etomoxir), or the glutaminase inhibitor (BPTES). Here, it is UK5099 to inhibit the mitochondrial pyruvate carrier. After six OCR readings, the remaining two compounds are added, and another six OCR readings are taken. The dependency is calculated as a percentage by dividing the loss of OCR following the target inhibitor (1) by the total loss of OCR with all three inhibitors present (2).

For the mitochondrial fuel capacity experiments, the compounds inhibiting alternative pathways would be added first, followed by the inhibitor for the target pathway.

### *Mitochondrial Fuel Flexibility Test:*

The mitochondrial fuel flexibility test is a combination of the mitochondrial fuel dependency test and another assay called the mitochondrial fuel capacity test that is used to determine the mitochondrial capacity when running on the fuel of interest. We ran the pyruvate flexibility test, using

the same assay setup as the mitochondrial fuel dependency assay, with UK5099 as the first compound added, and then etomoxir and UK5099 added as the second compounds. Other wells in the same plate are subjected to the etomoxir and BPTES first, followed by OCR measurements and then the UK5099. The capacity is then calculated as the inverse of the ratio of the baseline OCR minus the OCR with the other inhibitors over the baseline OCR minus the OCR following the target inhibitor (Figure 5).

#### Data Normalization:

OCR and ECAR values were normalized to cell number in each well. Plates of DAPI labeled cells were quantified using the Cytation5 microscope automated counting feature. Five images at 4x were taken per well. The average cell density of each image was obtained using measurements of the field of view, and the density was used to calculate the number of cells present in each well. Normalized OCR and ECAR data were analyzed in GraphPad Prism v. 9.

#### Statistical Analysis:

Unpaired two-tailed student's t-tests were used to compare control and stretched ONHAs; comparisons for which  $p \leq 0.05$  were considered statistically significant. Statistical analysis was done using GraphPad Prism 9.

## Proteomics Results

### *Upregulated Metabolic Proteins*

Stretched cortical astrocytes (CAs) had an altered proteome compared to control CAs, including increases in the glycolytic proteins aldolase fructose biphosphate c and the cytoplasmic enzyme isocitrate dehydrogenase-1 (IDH1) (Table 1,  $p=0.00065$  and  $p=0.022$  respectively). These proteins are both associated with the glycolytic pathway, with aldolase fructose biphosphate c being involved in splitting the 6-carbon fructose ring into dihydroxyacetone phosphate and d-glyceraldehyde-3-phosphate. IDH1 catalyzes the decarboxylation of isocitrate into  $\alpha$ -ketoglutarate, and in the process, reduces NADP<sup>+</sup> to NADPH. Interestingly, another enzyme that promotes the production of  $\alpha$ -ketoglutarate, glutamate dehydrogenase 1, was also significantly upregulated in stretched CAs (Table 1,  $p=0.00024$ ). Proteomics analysis yielded other increases in proteins associated with the TCA and  $\beta$ -oxidation cycles, such as acyl-CoA thioesterase 7, and acetyl-CoA acetyltransferase 2 (Table 1,  $p=0.039$  and  $p=0.041$  respectively). Acyl-CoA thioesterase 7 catalyzes hydrolysis of fatty acyl-CoAs to free fatty acids and coenzyme A, while acetyl-CoA acetyltransferase 2 can convert acetyl CoA to CoA and acetoacetyl CoA. CoA functions in the TCA cycle to regulate pyruvate dehydrogenase, or to aid in synthesis and transport of fatty acids.

### *Downregulated Metabolic Proteins*

Stretched CAs had lower expression of some metabolic proteins, particularly enzymes found in the first few steps of the TCA cycle. Citrate synthase and isocitrate dehydrogenase 2 (IDH2) are both significantly decreased in stretched CAs compared to control CAs (Table 1,  $p=0.013$  and  $p=0.027$  respectively). Citrate synthase catalyzes the production of citrate from oxaloacetate, the first step in the TCA cycle. Its activity is used as a proxy for mitochondrial mass. As mentioned above, IDH2 (found in the mitochondria) catalyzes the production of  $\alpha$ -ketoglutarate from isocitrate, a rate-limiting reaction in the

TCA cycle. Glycogen phosphorylase B, adenylate kinase 1, and hydroxyacyl-CoA dehydrogenase are all metabolism-associated proteins that are also downregulated in CAs (Table 1,  $p=0.001$   $p=0.0045$ , and  $p=0.028$  respectively). Glycogen phosphorylase B is the isoform of glycogen phosphorylase located in the CNS that is responsible for breaking down glycogen stores into glucose. Adenylate kinase 1 combines ATP and AMP into two molecules of ADP which can diffuse from areas of high ATP concentration to areas of low ATP concentrations. Adenylate kinase 1 also influences AMPK, which is a major regulator of cell metabolism. Hydroxyacyl-CoA dehydrogenase is located in the mitochondria, where it is part of the  $\beta$ -oxidation pathway, inhibiting glutamate dehydrogenase 1 (a protein we show upregulated in CAs). Decreases in inhibitory proteins leading to increases in their targets would be expected, and is one indication of the congruence of the proteomic findings.

#### *Lysosomal, Reactive, and Ribosomal Proteins*

Stretching the ONHAs affected the expression of more proteins than just metabolic proteins, such as proteins involved with autophagy, protein translation, and astrocyte reactivity. Lysosomal associated membrane protein 2 (LAMP2), a major lysosomal regulatory protein, is upregulated in stretched ONHAs (Table 1,  $p=0.012$ ). Adaptor related protein complex 2 subunit mu 1 is another lysosomal protein upregulated in stretched ONHAs (Table 1,  $p=0.027$ ); it is a vacuolar proton pump which is responsible for the acidification of lysosomes. A protein linked with the prominent astrocyte activation JAK-Stat3 pathway (Ceyzériat et al., 2016), hydroxysteroid 17-beta dehydrogenase 4, is upregulated in stretched ONHAs (Table 1,  $p=0.038$ ). pathway. Also increased in stretched ONHAs (Table 1,  $p=0.0041$ ) was cytochrome B5 type A, a protein that can transfer electrons from NADH for endoplasmic reticulum stress, ascorbate recycling, and is a target for cytochrome c on apoptotic release from the mitochondria. Stretching the ONHAs altered the expression of ribosomal proteins as well, with ribosomal protein S28 being upregulated (Table 1,  $p=0.031$ ), while ribosomal protein L7, ribosomal

protein L17, and ribosomal protein, large, P1 were all downregulated (Table 1,  $p=0.0078$ ,  $p=0.00037$ , and  $p=0.00056$ ).

Table 1: Proteomics Results			
Protein	Protein Function	P Value	Factor Change
Ribosomal Protein S28	Small subunit protein	0.031	+10
Heme Oxygenase 1	ROS regulatory protein	0.018	+10
Cytochrome b5 Type A	Membrane bound electron carrier	0.0041	+6
Adaptor related protein complex 2 subunit mu 1	Lysosomal proton pump	0.027	+5.5
Hydroxysteroid 17-beta dehydrogenase 4	JAK/STAT3 Activator Protein	0.038	+4.9
Acetyl-CoA acetyltransferase 2	Fatty Acid Oxidation	0.041	+3
Acetyl-CoA thioesterase 7	Peroxisomal protein, transports LCFA	0.039	+2.9
Aldolase, fructose-bisphosphate C	4 <sup>th</sup> enzyme in glycolysis	0.00065	+2.1
Glutamate dehydrogenase 1	Converts glutamate into $\alpha$ -ketoglutarate	0.00024	+2
Isocitrate Dehydrogenase 1	Converts isocitrate into $\alpha$ -ketoglutarate, cytoplasmic isoform	0.022	+2
Lysosomal associated membrane protein 2	Lysosomal marker needed to form lysosomes	0.012	+2
Citrate synthase	Converts oxaloacetate to acetyl-CoA, 1 <sup>st</sup> step in the TCA cycle	0.013	-2
Hydroxyacyl-CoA dehydrogenase	Mitochondrial inhibitor of glutamate dehydrogenase 1	0.028	-2
Ribosomal protein L7	Part of the large ribosomal subunit	0.0078	-2
Adenylate kinase 1	Converts ATP+AMP to 2ADP for metabolic homeostasis	0.0045	-2.5
Glycogen phosphorylase B	Breaks long term glycogen stores into glucose	0.001	-2.5
Ribosomal protein L17	Part of the large ribosomal subunit	0.00037	-3.333
Ribosomal protein, large, P1	Part of the large ribosomal subunit	0.00056	-3.333
Isocitrate dehydrogenase 2	Converts isocitrate into $\alpha$ -ketoglutarate, mitochondrial isoform	0.022	-10

## Metabolic Activity Experiments Results

### *Glycolytic Rate Assay*

A version of the glycolytic stress test was used to estimate the glycolytic rate in cells by measuring the changes in extracellular acidification rate (ECAR) following the addition of rotenone and antimycin-A to inhibit Complexes I and III, respectively, of the electron transport chain (Figure 6). Stretched optic nerve head astrocytes (ONHAs) showed no difference in their baseline ECAR compared to control ONHAs (data not shown,  $p=0.770$ ,  $n=20$ ). Due to the absence of glucose in the media, this extracellular acidification comes from cell processes other than glycolysis, mainly oxidative respiration (Wu et al., 2007; Mookerjee et al., 2015).

Stretched ONHAs had higher glycolytic ECAR values compared to control ONHAs from the addition of glucose during the Seahorse assay through the addition of 2-DG (Figure 6B,  $p=0.0037$ ,  $n=20$ ), suggesting that the stretched ONHAs are more glycolytically active than control astrocytes. Maximal ECAR, how much the cells can increase their glycolytic activity to produce ATP when mitochondrial respiration is inhibited, was significantly higher in stretched ONHAs compared to control ONHAs (Figure 6C,  $p=0.0039$ ,  $n=20$ ). Stretched ONHAs also had a higher glycolytic reserve than control ONHAs, as determined by subtracting their glycolytic ECAR from their maximal ECAR (Figure 6D,  $p=0.0136$ ,  $n=20$ ).

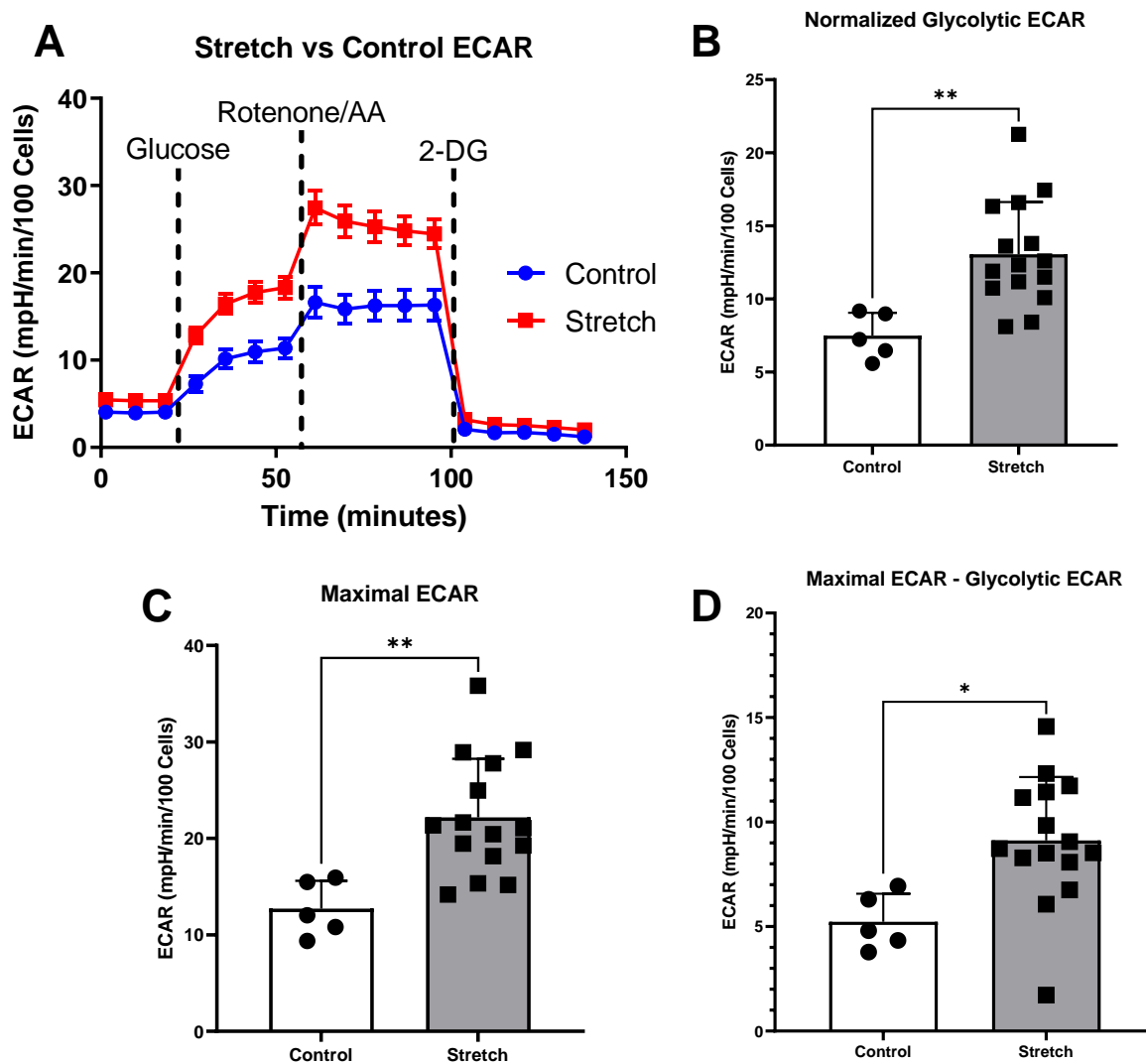


**Figure 6:** Glaucoma-like stretch causes an increase in glycolytic activity in primary optic nerve head astrocytes (ONHAs). A: Stretch increases the extracellular acidification rate (ECAR) of primary ONHAs. Measurements were taken every 9 minutes for baseline, glucose addition, rotenone and antimycin a, and 2-deoxyglucose (2-DG). B: Following the addition of glucose, stretched ONHAs have a significantly higher ECAR than control ONHAs ( $p=0.0037$ ,  $n=20$ ). C: Stretched ONHAs have a significantly higher maximal ECAR than control ONHAs ( $p=0.0039$ ,  $n=20$ ). D: Stretched ONHAs have a significantly higher ECAR upregulation following the addition of rotenone and antimycin-A compared to control ONHAs ( $p=0.0136$ ,  $n=20$ ).

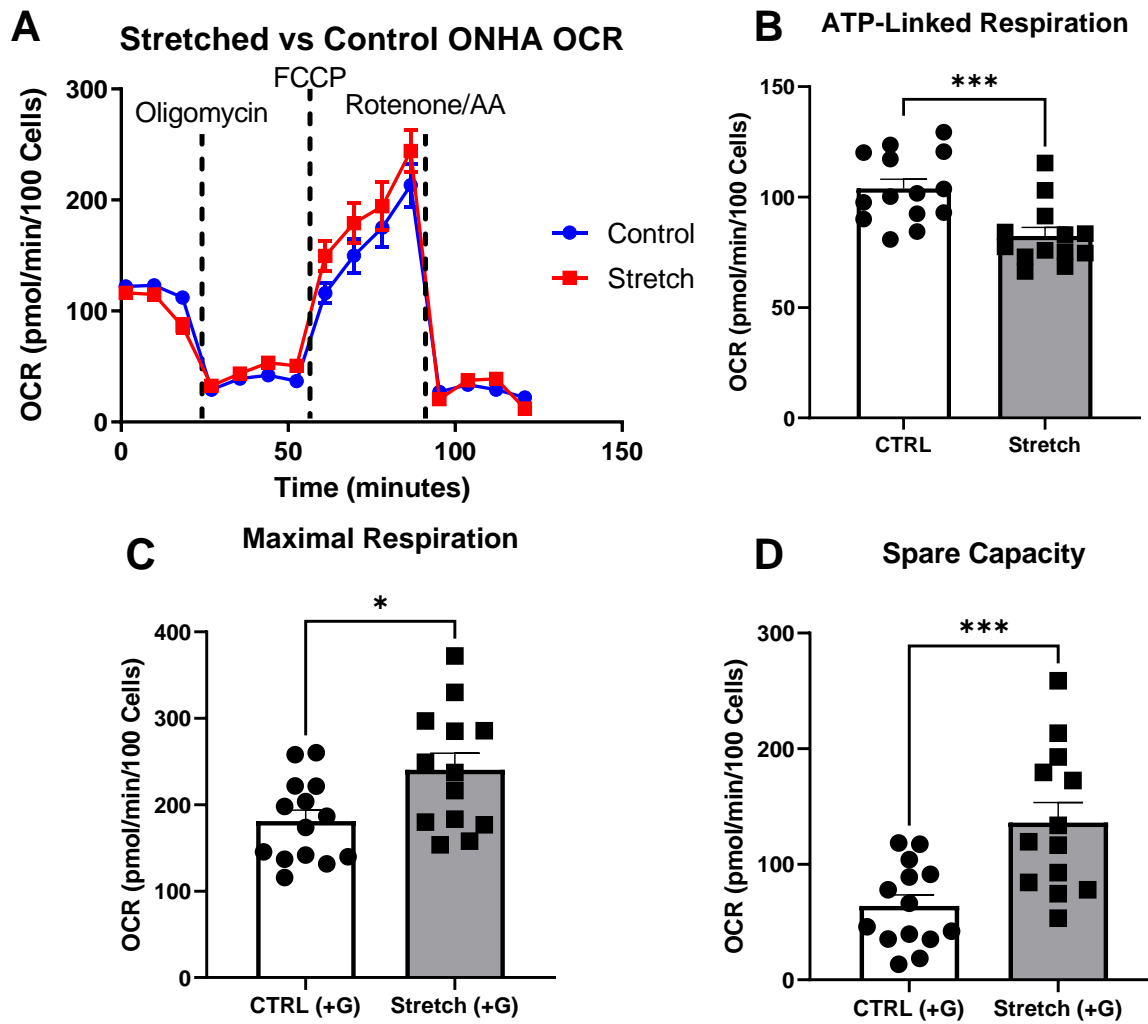


**Figure 7:** Optic Nerve Head Astrocytes (ONHAs) stretched as in glaucoma have altered mitochondrial respiration compared to control ONHAs. A: Stretched ONHAs have no difference in basal oxygen consumption rate (OCR). B: Stretched ONHAs have a higher ATP-linked mitochondrial OCR than control ONHAs ( $p=0.0009$ ,  $n=27$ ). C-D: Stretched ONHAs have a higher maximal respiration and spare capacity than control ONHAs ( $p=0.0157$ ,  $n=27$ ;  $p=0.0010$ ,  $n=27$ ).

### *Mitochondrial Stress Test*

The mitochondrial stress test uses electron transport chain complex inhibitors to challenge mitochondrial respiration as measured by oxygen consumption rate (OCR) in the Seahorse Analyzer. After baseline OCR is measured, inhibition of the ATP synthase using oligomycin-A enables us to calculate the oxygen attributable to ATP production. Next, FCCP, a protonophore that dissipates the mitochondrial membrane potential, forces maximal oxygen consumption as the electron transport chain (ETC) works to move electrons to restore the proton gradient; oxygen gets used as the terminal electron acceptor. Finally, a combination of rotenone and antimycin-A fully stops mitochondrial oxygen consumption by blocking Complexes I and III of the ETC; see explanatory schematic (Figure 4). OCR values for the cells were normalized to cell counts in each well (Figure 7A).

Stretched ONHAs had no difference in their basal respiration compared to control ONHAs. Stretched ONHAs had lower ATP-linked respiration compared to control ONHAs (Figure 7B,  $p=0.0009$ ,  $n=27$ ). Despite this difference in ATP-linked respiration, stretched ONHAs had higher maximal respiration (Figure 7C,  $p=0.0157$ ,  $n=27$ ) and higher spare capacity (Figure 7D  $p=0.0010$ ,  $n=27$ ), than control ONHAs. This suggests that the stretched ONHAs are able to be more responsive to metabolic challenges than control ONHAs.

### *Mitochondrial Fuel Dependency Test*

The mitochondrial fuel dependency test was used to determine how dependent the ONHA mitochondria are on three possible fuel sources: Pyruvate, glutamine, and long chain fatty acids (LCFAs). Compounds that can block transport or conversion of each of these fuel sources are used to observe how OCR changes under their influence. A large decrease in OCR after application of UK5099, the mitochondrial pyruvate carrier, for example, suggests pyruvate as an important source of mitochondrial fuel for ONHAs. Inhibitors of glutaminase for glutamine conversion to glutamate (BPTES), and carnitine palmitoyl-transferase 1A for LCFA translocation into the mitochondria for  $\beta$ -oxidation (etomoxir) were

used to evaluate dependence on glutamine and LCFAs, respectively (Figure 8A-C). There was no statistical difference between control and stretched ONHAs in their dependency on pyruvate, glutamine, or LCFAs. However, within groups, control ONHAs are more dependent on glutamine than on pyruvate, as are stretched ONHAs (Figure 8D,  $p=0.0180$ ,  $n=7$  and  $p=0.0243$ ,  $n=7$ ). Control ONHAs also were more dependent on glutamine than on LCFAs (Figure 8E,  $p=0.0158$ ,  $n=7$ ). There was no significant difference in stretched ONHA dependency on glutamine and LCFAs.

#### *Mitochondrial Fuel Flexibility Test*

Another method by which to understand ONHA metabolic function is to evaluate the capacity of mitochondria to use alternative fuels when certain fuel sources are denied them. To determine mitochondrial fuel capacity, two fuel pathways are inhibited (e.g., glutamine and LCFAs) while measuring OCR, followed by inhibition of the target pathway (e.g., pyruvate). We tested the mitochondrial capacity for pyruvate since the dependency data suggested the control and stretched ONHAs were more dependent on glutamine. There was no difference in the capacity of control and stretched ONHAs to use pyruvate (Figure 9B). The difference in fuel capacity and dependency, also known as fuel flexibility, was no different between control and stretched ONHAs for pyruvate (Figure 9C).

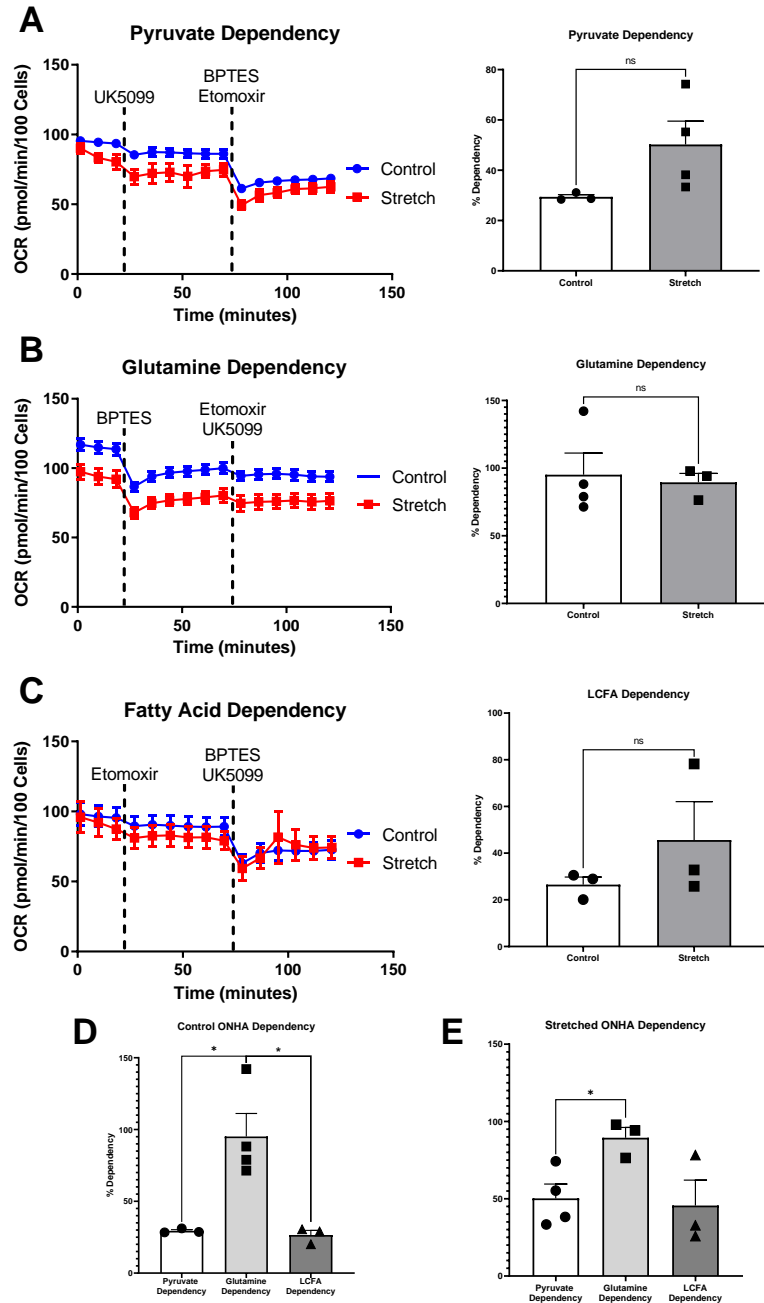


**Figure 8:** Mitochondrial substrate preference of optic nerve head astrocytes (ONHAs) is not changed by glaucomic stretch. A-C: Oxygen consumption rates (OCRs) tested for pyruvate (A), glutamine (B), and fatty acid metabolic dependency (C) are not different between stretched and control ONHAs. D-E: Control ONHAs (D) depend more glutamine than on pyruvate and fatty acids for their mitochondrial respiration, while Stretched ONHAs depend more on glutamine

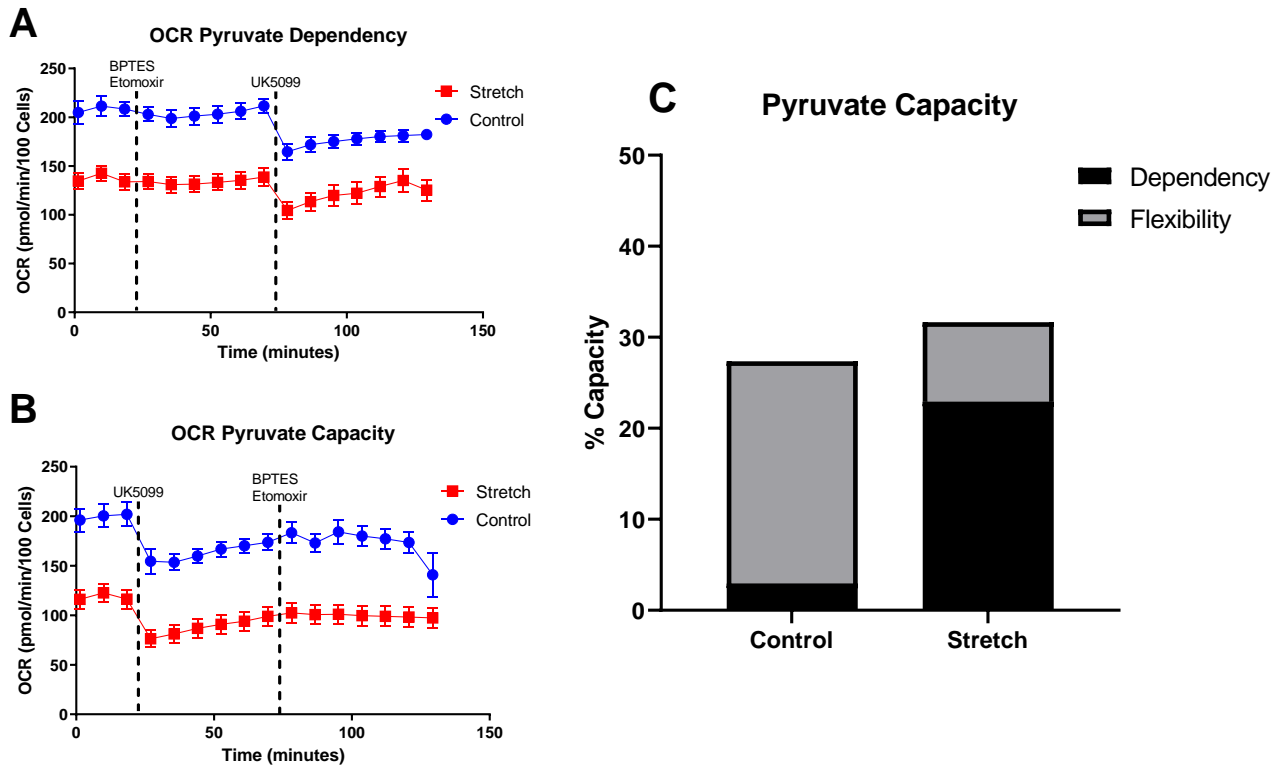


**Figure 9:** Stretched ONHAs and control ONHAs had no difference in mitochondrial pyruvate flexibility. (A) Stretched and control ONHA OCR in the pyruvate dependency assay. (B) Stretched and control ONHA capacity in the pyruvate capacity assay. (C) There was no difference between stretched and control ONHA pyruvate flexibility.

## Discussion

### *Stretched astrocyte metabolic proteome differs from control astrocytes*

The proteomic experiments comparing stretched and control cortical astrocytes (CAs) reveal a shift towards more glycolytic ATP production but also  $\beta$ -oxidation. Additionally, the proteomics show a decrease in proteins associated with the TCA cycle.

Aldolase fructose bisphosphate c is an aldolase enzyme that catalyzes the reversible reaction between fructose-1,6-bisphosphate to glyceraldehyde and dihydroxyacetone phosphate, the fourth step in glycolysis. Cytochrome b5 type A receives electrons from the NADH generated by glycolysis and ferries the electrons into the ETC. These upregulated proteins power portions of the glycolytic pathway by metabolizing glucose and utilizing the NADH generated, corroborating glycolysis increases that we confirm with our bioenergetic experiments. These glycolytic proteome increases are also supported by the increase in glycolytic ECAR and maximal ECAR following rotenone/antimycin-A that we observed in our modified glycolytic stress test. However, it is interesting that the main proteins responsible for glycolytic regulation (glucose transporter 1 (GLUT1), hexokinase, phosphofructokinase and monocarboxylate transporter-1 (MCT1) (Tanner et al., 2018)) are neither upregulated nor downregulated in this proteomic analysis. Astrocytes are primarily glycolytic (Bélanger et al., 2011; Turner and Adamson, 2011), and it may be the case that these glycolysis-associated transporters and enzymes could already be expressed at a high enough level to support increased glycolysis in the stretched ONHAs. This is contrary to data we have published showing decreases in GLUT1 and MCT1 in glaucomic ON, including ONH (Harun-Or-Rashid et al., 2018). However, a potential explanation is the difference in the acute stretch injury we are subjecting the cortical astrocytes to instead of the chronic changes and degeneration in glaucoma. Further, GLUT1 expression is regulated by HIF-1 $\alpha$ , the transcription factor stabilized by hypoxia. Despite demonstrating hypoxia in the D2 mouse model of glaucoma, chronic HIF-1 $\alpha$  expression no longer has the same impact on glycolysis upregulation, a

condition known as pseudohypoxia. Pseudohypoxia explains the lack of GLUT1 upregulation despite HIF-1 $\alpha$  expression in the D2 retina. Evidence in the D2 suggests pseudohypoxia may be the result of a breakdown in the communication between the nucleus and mitochondria (Jassim et al, 2021).

There are a series of proteins increased in the stretched cortical astrocytes that point to an increase in  $\beta$ -oxidation alongside an increase in glycolytic activity. Glutamate dehydrogenase 1 and isocitrate dehydrogenase-1 are used to produce  $\alpha$ -ketoglutarate (Reitman and Yan, 2010; Plaitakis et al., 2017) while acetyl-CoA acetyltransferase 2 and acyl-CoA thioesterase 7 are used for fatty acid degradation in the cytoplasm and peroxisome. These molecules support peroxidation in cells, the breakdown of long chain fatty acids (LCFAs) to a length where mitochondria can oxidize them. Peroxidation produces FADH<sub>2</sub> which donates its electrons to O<sub>2</sub> to produce H<sub>2</sub>O<sub>2</sub> instead of donating its electrons to the ETC (Rose et al., 2020). This evidence of fatty acid peroxidation could explain the lowered ATP-production linked oxygen consumption rate (OCR) expressed in stretched optic nerve head astrocytes (ONHAs), as well as provide insight into how their maximal and reserve OCR are increased compared to control ONHAs as they are consuming oxygen to prepare fatty acids for ATP production instead of using oxygen for ATP production directly. The breakdown of LCFAs is done oxidatively in the peroxisomes, mitochondria, and ER to produce acetyl-CoA for the mitochondria, using oxygen while producing ATP indirectly through their own malate-aspartate shuttles to transfer their oxidizing molecules out of the peroxisome. Once acetyl-CoA is transported into the mitochondria by carnitine palmitoyltransferase I, it undergoes oxidative phosphorylation through the TCA cycle.

Stretched CAs have decreased expression of two of the most important proteins in the TCA cycle, citrate synthase and isocitrate dehydrogenase-2. Citrate synthase is used to turn oxaloacetate into citrate, the point where the TCA cycle begins again after oxaloacetate has donated its last electrons. Isocitrate dehydrogenase-2 is the mitochondrial isoform of isocitrate dehydrogenase, and it turns D-isocitrate into  $\alpha$ -ketoglutarate, donating the first electrons in a rotation of the TCA cycle. The enzymatic

activity of either of these proteins can be used to estimate/measure mitochondrial activity, and their downregulation in stretched CAs point to an altered TCA cycle compared to control CAs. The differences observed here in the mitochondrial and cytoplasmic isoforms of isocitrate dehydrogenase (2 and 1 respectively) suggest a further increased importance of the malate-aspartate shuttle other than replenishing NAD<sup>+</sup> for glycolytic function. An increase in  $\alpha$ -ketoglutarate could also be used to maintain the TCA cycle and oxidative ATP production, which could be tested with a metabolomics experiment comparing the metabolome of stretched and control ONHAs. Increases in isocitrate dehydrogenase 1 have also been linked to deficiencies in the malate-aspartate shuttle in the past (Gaude et al., 2018; Borst, 2020). Cells with the malate aspartate shuttle shut off have been shown to take glutamine, convert it into glutamate which is then transaminated to make 2-oxoglutarate which isocitrate dehydrogenase 1 converts to isocitrate using NADH. This produces NAD<sup>+</sup> that is necessary for glycolytic function when the malate/aspartate shuttle system is not producing enough.

Increases in glycolysis and  $\beta$ -oxidation provide increased energy to stretched CAs, but they do not tell us what this energy is being used for, or where the byproducts are going. Based on the increase in glycolytic ECAR and decreased TCA cycle activity, it may be the case that the stretched astrocytes are exporting more lactate than they are consuming pyruvate. The increase observed in  $\beta$ -oxidation proteins could be a compensatory method for the lowered citrate synthase and isocitrate dehydrogenase-2 to support the TCA cycle and mitochondrial respiration. Based on other proteins that are upregulated in stretched CAs such as hydroxysteroid 17-beta dehydrogenase 4 (the mitochondrial matrix protein that regulates glutamate dehydrogenase), heme oxygenase 1 (a reactive oxygen species regulator) and lysosomal associated membrane protein 2 (a lysosomal indicator, the organelles responsible for recycling autophagic proteins), it appears that the stretched CAs are stressed and likely to enter a period of reactivity.

*Stretched Optic Nerve Head Astrocytes Had Altered Glycolytic Profiles from Control Cells*

The increase in glycolytic activity shown by the modified glycolytic stress test suggests that the stretched optic nerve head astrocytes (ONHAs) are shifting towards a more glycolytic energy profile than control ONHAs. It should be noted that there are some caveats to this experiment. To begin with, while I had a sufficient  $n$  value to obtain statistically significant data, the results could be made stronger with additional biological replicates, particularly in the control group. Additionally, I used a combination of rotenone and antimycin-A to halt mitochondrial ATP production instead of oligomycin. Rotenone and antimycin-A are complex I and complex III inhibitors respectively. Stopping these complexes in the electron transport chain (ETC) does stop the oxygen consumption in the mitochondria, but it does not immediately stop the mitochondrial ATP production. This is because the leftover proton gradient after stopping the ETC can still power the ATP-synthase in the mitochondria, allowing the organelle to continue producing ATP for a time after the stopping of the ETC. The traditional glycolytic stress test uses oligomycin (an ATP-synthase inhibitor) as its second compound addition to determine the maximal extracellular acidification rate (ECAR) attributable to glycolytic ATP production as glycolysis is the major remaining ATP source following ATP-synthase inhibition. Trial experiments using oligomycin found no large increase in ECAR following oligomycin addition, and I was then directed to the glycolytic rate assay, another experimental procedure to estimate glycolytic activity. This experiment used rotenone and antimycin-a as their second compound to determine their maximal glycolytic rate, and I assumed I could use that combination as the mitochondrial inhibitor for the glycolytic stress test. I missed the outcome measures for these two experiments and made my data wonky as a result. The glycolytic rate assay used proton emission rate (PER) as its outcome measure (instead of ECAR), which requires careful buffering of the assay media and blank control wells on the Seahorse culture plate. By not buffering my media, and adding the glucose to the assay as it was underway, I could not know the buffering capacity of my assay media, so I could not use the known ECAR to calculate the PER. Future experiments to finalize my

glycolytic rate data will be done using the proper buffering in the media and the traditional glycolytic rate assay.

Aside from the caveats stated above, I can say that the stretched ONHAs have a higher baseline glycolytic activity than control ONHAs as measured by the ECAR attributable to glycolysis. This means that the cells are undergoing more glycolysis, presumably for the increased ATP production for the stressed stretched cells, but glycolysis has other uses as well. Glycolysis can feed into the pentose phosphate pathway and then into glutathione generation, a molecule used for controlling reactive oxygen species (ROS). ROS production has been shown in the literature to be increased in reactive astrocytes (Sheng et al., 2013; Vicente-Gutiérrez et al., 2021), so increased glutathione from the pentose phosphate pathway might be one of the mechanisms for managing ROS. Another way the ONHAs could be regulating an increase in ROS production could come from the increase in heme oxygenase 1 we observed in our proteomics experiment. Heme oxygenase 1 is an enzyme that regulates proteins that protect cells against ROS, such as superoxide dismutase and glutathione. Its increase here could be using these two methods to protect the stretched ONHAs against potential ROS production with increased fatty acid oxidation. Glycolysis can also produce lactate, which astrocytes can use to fuel/support the neurons they are in contact with (Pellerin et al., 1998; Volkenhoff et al., 2015; Muraleedharan et al., 2020). Lactate can also be converted into pyruvate for mitochondrial consumption by lactate dehydrogenase. There are five different isozymes of this protein, all made up of different compositions of the subunits LDHA and LDHB. The kinetics of the LDHB subunit favors conversion of lactate into pyruvate, while the LDHA subunit converts pyruvate into lactate (O'Brien et al., 2007). Astrocytes have been shown to express more LDHA subunits than LDHB, suggesting that the pyruvate produced by glycolysis in astrocytes is converted into lactate and shuttled to neurons, where the LDHA subunits preferentially converts lactate into pyruvate for use in the mitochondria (Bittar et al., 1996; Laughton et al., 2000).

Future work investigating the glycolytic activity of stretched ONHAs could investigate the lactate production and transport in stretched ONHAs. This is particularly interesting as we see that ON taken from glaucomic mice show an inability to upregulate their glycolysis when challenged, in addition to decreased glucose transporter and monocarboxylate transporter (MCT) expression compared to control mice. This would be a discrepancy if we found that the increased glycolytic and maximal ECAR in stretched ONHAs occurred without decreases in glucose transporters or MCTs. Decreased glucose transporters in glaucomic ON suggest that the cells are not able to obtain as much glucose as would be necessary to support this increase in glycolysis that we observe, and a decrease in MCTs would inhibit the release of lactate and protons from the astrocytes, thus lowering the ECAR measurements. Changes in connexin-43, the primary gap junction protein in astrocytes, could also affect glycolysis in glaucomic ON. *In vitro* experiments have shown that both hydrostatic pressure and oxygen/glucose deprivation and reperfusion experiments lead to decreases and relocation of connexin-43 intracellularly (Malone et al., 2007; Xie et al., 2017), potentially reducing the spread of glucose between astrocytes for glycolytic function. It is possible that the changes that we observe in the stretched ONHAs are acute changes, and that the metabolism of ONHAs changes yet again during glaucoma as it is a chronic optic neuropathy. Isolating ONHAs from *in vivo* glaucoma models would allow us to confirm the observed glycolytic changes with a chronically stressed/stretched astrocyte population. A final consideration is that the changes observed in glaucoma have been in full ON, with the ONH included. The ONH is only a small part of the nerve as a whole, so its changes could get washed out by the increased amount of RGC axons present, or even the oligodendrocytes (which also express GLUT1 and MCT1).

#### *Stretched Optic Nerve Head Astrocytes' Mitochondria Are More Responsive Than Control Cells*

Stretched ONHAs showed increased maximal respiratory rates and spare capacities compared to control ONHAs. This difference is interesting as we observed no difference in the baseline mitochondrial OCRs in stretch and control ONHA groups. Additionally, the decrease in citrate synthase and isocitrate

dehydrogenase-2 would suggest that the TCA cycle would be more reliant on  $\alpha$ -ketoglutarate in stretched ONHAs. It appears that the stretched ONHAs are making up for this decreased citrate synthase and isocitrate dehydrogenase 2 presence and ATP-linked respiration with fatty acid oxidation and potentially with  $\alpha$ -ketoglutarate production.

Fatty acid oxidation is the process by which cells break down fatty acids to produce acetyl-CoA for entry into the TCA cycle and mitochondrial respiration. We see increases in the proteins acetyl-CoA thioesterase 7 and acetyl-CoA acetyltransferase which are important for fatty acid oxidation in the peroxisomes, and the generation of acetyl-CoA. This could be a change in the mitochondrial fuel source following stretch, or just another fuel source for them. The increase in maximal respiration and spare capacity shows that the stretched cells are more metabolically responsive than the control ONHAs, similarly to the increased maximal glycolytic ECAR. These cells might be becoming more responsive to their environment in their reactive state. These might additionally be pathways that are increased in reactive astrocytes, which we know have increased fatty acid metabolism (Zamanian et al., 2012; Liddelow et al., 2017).

#### *Stretched Optic Nerve Head Astrocytes Had No Changes in Mitochondrial Fuel Dependency*

The mitochondrial fuel dependency test uses a combination of three mitochondrial transporter inhibitors to test the mitochondria's dependency on those three fuel sources. BPTES is used to block glutaminase and glutamine metabolism, UK5099 is used to block the mitochondrial pyruvate carrier (MPC) and pyruvate metabolism, and etomoxir is used to block carnitine transferase and LCFA metabolism. We showed no difference in the mitochondrial dependency for these three fuel sources in stretched and control ONHAs. We did show that ONHAs are more dependent on glutamine than pyruvate, and that control ONHAs are more reliant on glutamine than LCFAs. Glutamine metabolism produces glutamate, which then makes  $\alpha$ -ketoglutarate which can enter the TCA cycle, or produce electron carrying molecules in the malate/aspartate shuttle. Increased fatty acid oxidation proteins and

the astrocytic preference for glutamine over pyruvate as a mitochondrial fuel source reinforces the lactate-shuttle hypothesis as the astrocytes do not rely on pyruvate for mitochondrial respiration which allows them to export lactate for neuronal consumption. The major caveat to this data set is that the experiment needs to be replicated. The assay is run with all three inhibitor combinations run in the same plate, giving each of the six groups a particularly small  $n$  value. This experiment needs to be replicated to determine the accuracy of the data, particularly as there appears to be a non-significant difference in the groups that may prove to be significant with appropriate replicate experiments. Seahorse experiments are traditionally run in triplicate to ensure the accuracy of run data, so this experiment needs to be replicated twice to ensure there is no difference in mitochondrial fuel dependency between stretched and control ONHAs.

Working with the data as it is presented, it is possible that there is indeed no difference in the mitochondrial fuel dependency in stretched and control ONHAs. This could be because astrocytes are preferentially glycolytic and are more reliant on glucose for their ATP production than on mitochondrial respiration (Dienel and Hertz, 2001; Turner and Adamson, 2011). The observed increase in maximal respiration in the stretched ONHAs could be supported by the mitochondrial transport proteins that are also present in control ONHAs. Future experiments measuring the expression of the transporter proteins that are blocked by the inhibitors in the mitochondrial fuel dependency test (glutaminase 1, MPC, and carnitine transferase 1) could support future mitochondrial fuel dependency experiments. It should also be considered that short chain fatty acids (SCFAs) are another major mitochondrial fuel source that are not brought into the mitochondria by transporters. As small lipids, SCFAs can pass through the phospholipid bilayers in the mitochondria freely. As a mitochondrial fuel source,  $\alpha$ -ketoglutarate is particularly interesting. It is a mitochondrial fuel source, an alpha keto acid that might be more concentrated in stretched ONHAs than control ONHAs as they have increases in glutamate dehydrogenase and isocitrate dehydrogenase-1, which both catalyze reactions that produce  $\alpha$ -

ketoglutarate. The preference of ONHAs for glutamine over pyruvate and LCFAs also suggest an increased role for glutamine as its metabolism produces glutamate and ultimately  $\alpha$ -ketoglutarate for mitochondria to use as fuel. Our experiments suggest an increased role for  $\alpha$ -ketoglutarate in stretched ONHAs.

#### *Stretched Optic Nerve Head Astrocytes Are Not More Flexible with Pyruvate Than Control Cells*

The mitochondrial fuel flexibility assay is an assay that tests how cells alter their mitochondrial respiration and support it using one substrate of interest. We ran this experiment testing pyruvate dependency/flexibility on the assumption that as stretched ONHAs become more glycolytic, there would be an increase in pyruvate availability. The assay runs a mitochondrial fuel dependency assay as previously described, but only for the mitochondrial pyruvate carrier (MPC). We showed no difference in pyruvate dependence in stretched and control ONHAs, an unsurprising result because we have shown increases in glycolysis but a decrease in the enzymes that bring pyruvate's products into the TCA cycle, citrate synthase and isocitrate dehydrogenase-2. We have also shown no difference in pyruvate dependency when comparing stretched and control ONHAs.

The inability of ONHAs to maintain their mitochondrial respiration relying on pyruvate could be interesting given our understanding of astrocyte metabolism. Astrocytes have been shown in the past to be glycolytic, even though they have extensive mitochondrial networks (Rahman and Suk, 2020). It could be thought that as the stretched ONHAs become more glycolytic, there is an increased concentration of pyruvate which can be taken up by pyruvate dehydrogenase before it is shuttled from the cell, but this does not appear to be the case. This seems to lend more credence to the lactate shuttle hypothesis, which states that astrocytes produce lactate for export to neurons to use as mitochondrial fuel following the conversion to pyruvate.

This experiment will need to be replicated to be fully confident in the results, as this experiment has been run only once instead of in triplicate. We have more confidence in these results than in the

mitochondrial fuel dependency assay results as the pyruvate dependency data from that assay is in line with the pyruvate dependency data from this experiment, and this coincides with the decrease in citrate synthase in stretched cortical astrocytes. Replicates of the mitochondrial fuel dependency assay will allow us to better determine changes in the dependency of these mitochondrial substrates and give us a more solid understanding of mitochondrial respiration in stretched ONHAs before attempting more mitochondrial fuel flexibility assays.

#### *$\alpha$ -ketoglutarate Changes in Optic Nerve Head Astrocytes and Their Significances*

One molecule with metabolic significance that has been present in the proteomics experiments and in the Seahorse assays is  $\alpha$ -ketoglutarate. The proteomics experiments point to  $\alpha$ -ketoglutarate as it is produced in the cytoplasm by isocitrate dehydrogenase-1 and mitochondrially by glutamate dehydrogenase-1. Additionally, stretched ONHAs see a decrease in hydroxyacyl-CoA dehydrogenase, which negatively regulates glutamate dehydrogenase 1, making it more active in turn. The increase in maximal respiration in stretched ONHAs paired with the lack of changes in mitochondrial fuel dependency in stretched and control ONHAs suggests that there may be another mitochondrial fuel source at play that is responsible for these changes, such as the alpha keto acid  $\alpha$ -ketoglutarate. Several biochemical pathways make use of  $\alpha$ -ketoglutarate, but the two most interesting to consider for stretched ONHA metabolism are the TCA cycle, and the malate-aspartate shuttle. These pathways are both metabolically important and have broad implications for the metabolic activity in stretched ONHAs.

The TCA cycle uses  $\alpha$ -ketoglutarate in the fifth step of the pathway to make NADH and succinyl-CoA. Succinyl-CoA goes on through the remainder of the TCA cycle and makes more NADH for the electron transport chain (ETC) to maintain the proton gradient that powers mitochondrial ATP-synthase. The increases in glutamate dehydrogenase and decrease in citrate synthase suggest that  $\alpha$ -ketoglutarate may be a way for new substrates to enter the TCA cycle in stretched ONHAs that is less utilized in control ONHAs.

The malate-aspartate shuttle is a biochemical system for transporting malate out of the mitochondria when the TCA cycle is finished, and a way to replenish cytoplasmic NAD<sup>+</sup> concentrations following glycolysis. The important reaction in this shuttle for  $\alpha$ -ketoglutarate is the malate- $\alpha$ -ketoglutarate antiporter found on the inner membrane of the mitochondria. This protein exchanges malate and  $\alpha$ -ketoglutarate to maintain the shuttle. Increased production of  $\alpha$ -ketoglutarate might suggest an increase in this shuttle, as we also see a decrease in citrate synthase in the stretched cortical astrocytes. Citrate synthase combines oxaloacetate and acetyl-CoA to make citrate, the starting molecule in the TCA cycle and a way to recycle the oxaloacetate which is the final product of the TCA cycle. The observed decrease in the recycling enzyme of oxaloacetate and the increase in  $\alpha$ -ketoglutarate associated proteins suggests that this could be a way that cells are increasing their mitochondrial respiration and glycolytic rates at the same time. Finally, as stated earlier, the increase in isocitrate dehydrogenase 1 could combine with the astrocyte's dependency on glutamine to support their glycolytic activity by providing increased NAD<sup>+</sup> to the cytosol for glycolysis.

Future experiments into the role of  $\alpha$ -ketoglutarate in stretched ONHA metabolism could further our understanding of its role in regulating ONHA metabolism. It can be measured using biochemical assay, allowing for the measurement of  $\alpha$ -ketoglutarate concentrations in stretched and control ONHAs. Confirming that  $\alpha$ -ketoglutarate is upregulated is important for this interpretation. The effect of the malate-aspartate shuttle on stretched ONHA metabolism could be tested using aminooxyacetic acid, a common inhibitor of the malate-aspartate shuttle. This molecule inhibits aspartate aminotransferase which converts glutamate into  $\alpha$ -ketoglutarate in the mitochondrial matrix and the intermembrane space. By blocking this conversion,  $\alpha$ -ketoglutarate and glutamate cannot be replenished to maintain either the malate- $\alpha$ -ketoglutarate antiporter or the glutamate-aspartate antiporter that are both needed for the malate-aspartate shuttle, and the generation of NAD<sup>+</sup> for glycolysis.

## Conclusion

Compared to control, stretched cortical astrocytes have altered metabolic protein expression. Proteins related to glycolytic activity (such as aldolase fructose-bisphosphate C and isocitrate dehydrogenase 1) and proteins related to fatty acid oxidation (such as acetyl-CoA acetyltransferase 2 and acetyl-CoA thioesterase 7) are significantly increased. In addition, there are decreases in metabolic proteins relating to the TCA cycle (citrate synthase and isocitrate dehydrogenase 2) and the protein glycogen phosphorylase B. The decrease of citrate synthase and isocitrate dehydrogenase 2 suggests that there may be decreased turnover within the TCA cycle, and that oxaloacetate could be entering the malate/aspartate shuttle to support increased glycolytic activity in stretched cortical astrocytes. Glycogen phosphorylase B is the primary enzyme that breaks down the long-term energy stores of glycogen into glucose, and its loss suggests that the glycogen stores have been used up, as we see in glaucomic ON.

Stretched ONHAs have increased glycolytic activity compared to control ONHAs. This could indicate increased lactate export for neuronal support, or decreased lactate export/metabolic support; greater insight will only be obtained via future studies into the proteomes of the stretched ONHAs. If the metabolic transport channels are not altered, the stretched ONHAs could be exporting lactate at a higher rate than control cells, but if the metabolic transporters are decreased like we see in glaucomic ON tissue, the cells could be using the increased glycolysis for the pentose phosphate pathway, or for the total oxidation of pyruvate in stretched conditions. The increase in maximal OCR and spare capacity in the mitochondrial stress test suggests that while there is no difference in basal OCR and a decrease in ATP-linked respiration in stretched ONHAs, the cells are more prepared to work through metabolic challenges than control cells.

We can conclude from our proteomics experiments and the metabolic investigations that stretching astrocytes increases their glycolytic activity. This change could be beneficial to the neurons these astrocytes support, or detrimental as we will determine with future studies into the proteome of stretched ONHAs, and protein changes in metabolic proteins in stretched ONHAs and cortical astrocytes. These studies will expand on the information presented here to develop our understanding of the metabolic changes in ONHAs, and the impacts these changes have on glaucoma.

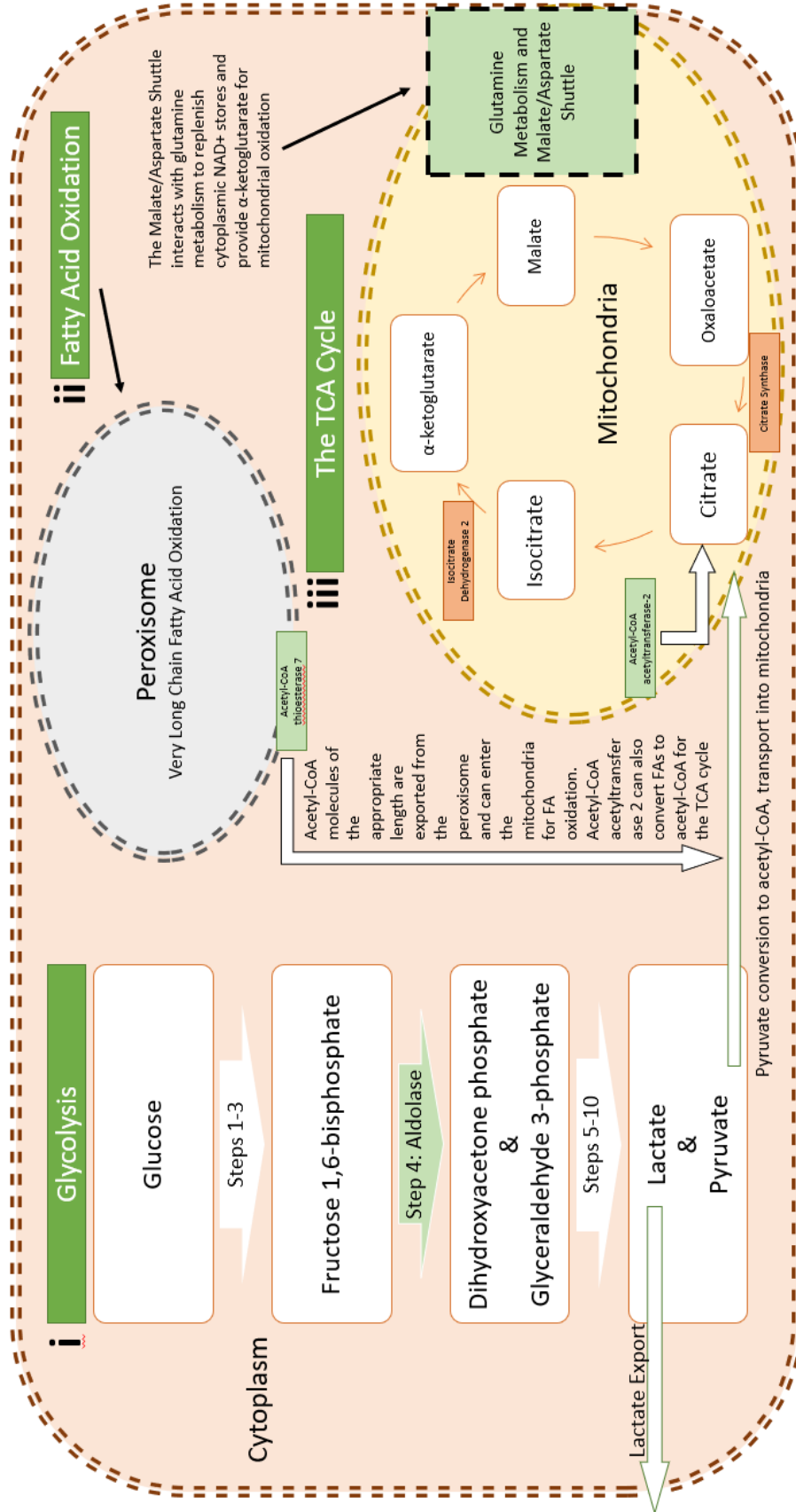


**Figure 10: Metabolic Pathways Altered in Stretched Optic Nerve Head Astrocytes (ONHAs):** Proteins highlighted in green are upregulated and proteins highlighted in orange are downregulated, as in Table 1. (i) Glycolysis is upregulated in stretched ONHAs, as aldolase fructose-bisphosphate c is upregulated alongside cytoplasmic proteins responsible for providing NAD<sup>+</sup> to glycolysis. (ii) Fatty Acid (FA) oxidation proteins are increased in stretched ONHAs, shown here. (iii) TCA proteins (citrate synthase and isocitrate dehydrogenase 2), as well as those related to recycling oxaloacetate are downregulated in stretched ONHAs.

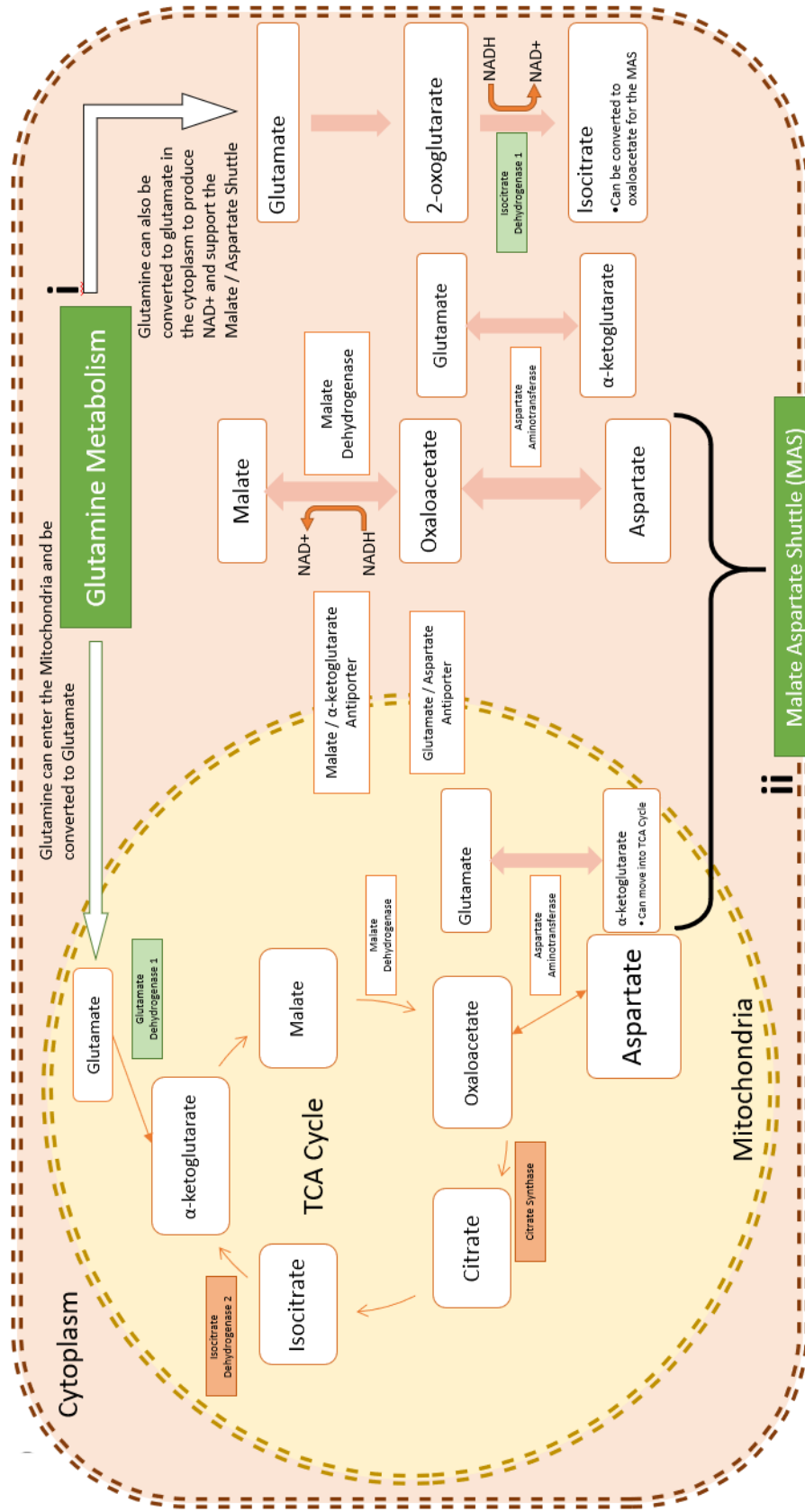


**Figure 11:** *Changes in Glutamine and  $\alpha$ -ketoglutarate in Stretched Optic Nerve Head Astrocytes (ONHAs):* Proteins highlighted in green are upregulated and proteins highlighted in orange are downregulated, as in Table 1. (i) Glutamine metabolic proteins are increased in stretched ONHAs, such as glutamate dehydrogenase 1 and isocitrate dehydrogenase 1, showing the importance of glutamine as a mitochondrial fuel source. (ii) The Malate/Aspartate shuttle is of particular interest to us with regard to glycolytic and TCA cycle maintenance as it can provide  $\alpha$ -ketoglutarate to the TCA cycle, provide NAD<sup>+</sup> to the cytoplasm for glycolysis, and be an endpoint for glutamine metabolism in stretched ONHAs.

## References

Albalawi F, Lu W, Beckel JM, Lim JC, McCaughey SA, Mitchell CH (2017) The P2X7 receptor primes IL-1 $\beta$  and the NLRP3 inflammasome in astrocytes exposed to mechanical strain. *Front Cell Neurosci* 11:227 Available at: [www.frontiersin.org](http://www.frontiersin.org) [Accessed March 25, 2021].

Allaman I, Gavillet M, Bélanger M, Laroche T, Viertl D, Lashuel HA, Magistretti PJ (2010) Amyloid- $\beta$  aggregates cause alterations of astrocytic metabolic phenotype: Impact on neuronal viability. *J Neurosci* 30:3326–3338 Available at: <https://www.jneurosci.org/content/30/9/3326> [Accessed March 10, 2021].

Amaral AI, Teixeira AP, Martens S, Bernal V, Sousa MFQ, Alves PM (2010) Metabolic alterations induced by ischemia in primary cultures of astrocytes: Merging <sup>13</sup>C NMR spectroscopy and metabolic flux analysis. *J Neurochem* 113:735–748 Available at: <https://pubmed.ncbi.nlm.nih.gov/20141568/> [Accessed March 10, 2021].

Anderson MG, Smith RS, Hawes NL, Zabaleta A, Chang B, Wiggs JL, John SWM (2002) Mutations in genes encoding melanosomal proteins cause pigmentary glaucoma in DBA/2J mice. *Nat Genet* 30:81–85 Available at: <https://www.nature.com/articles/ng794> [Accessed February 17, 2021].

Baltan S, Inman DM, Danilov C, Morrison RS, Calkins DJ, Horner PJ (2010) Metabolic vulnerability disposes retinal ganglion cell axons to dysfunction in a model of glaucomatous degeneration. *J Neurosci* 30:5644–5652.

Bélanger M, Allaman I, Magistretti PJ (2011) Brain Energy Metabolism: Focus on Astrocyte-Neuron Metabolic Cooperation. *Cell Metab* 14:724–738 Available at: <https://www.sciencedirect.com/science/article/pii/S1550413111004207#fig1> [Accessed October 1, 2019].

- Berry RH, Qu J, John SWM, Howell GR, Jakobs TC (2015) Synapse loss and dendrite remodeling in a mouse model of glaucoma. *PLoS One* 10:e0144341 Available at: <http://dx.doi.org/10.7910/> [Accessed March 23, 2021].
- Bittar PG, Charnay Y, Pellerin L, Bouras C, Magistretti PJ (1996) Selective distribution of lactate dehydrogenase isoenzymes in neurons and astrocytes of human brain. *J Cereb Blood Flow Metab* 16:1079–1089 Available at: <https://pubmed.ncbi.nlm.nih.gov/8898679/> [Accessed March 22, 2021].
- Borst P (2020) The malate–aspartate shuttle (Borst cycle): How it started and developed into a major metabolic pathway. In: *IUBMB Life*, pp 2241–2259. Blackwell Publishing Ltd. Available at: </pmc/articles/PMC7693074/> [Accessed March 26, 2021].
- Buckingham BP, Inman DM, Lambert WS, Oglesby E, Calkins DJ, Steele MR, Vetter ML, Marsh-Armstrong N, Horner PJ (2008) Progressive ganglion cell degeneration precedes neuronal loss in a mouse model of glaucoma. *J Neurosci* 28:2735–2744.
- Ceyzériat K, Abjean L, Carrillo-de Sauvage M-A, Ben Haim L, Escartin C (2016) The complex STATes of astrocyte reactivity: How are they controlled by the JAK–STAT3 pathway? *Neuroscience* 330:205–218 Available at: <https://www.sciencedirect.com/science/article/pii/S0306452216302020#f0005> [Accessed August 21, 2018].
- Chidlow G, Ebnetter A, Wood JPM, Casson RJ (2011a) The optic nerve head is the site of axonal transport disruption, axonal cytoskeleton damage and putative axonal regeneration failure in a rat model of glaucoma. *Acta Neuropathol* 121:737–751 Available at: <http://link.springer.com/10.1007/s00401-011-0807-1> [Accessed October 18, 2020].
- Chidlow G, Ebnetter A, Wood JPM, Casson RJ (2011b) The optic nerve head is the site of axonal transport

disruption, axonal cytoskeleton damage and putative axonal regeneration failure in a rat model of glaucoma. *Acta Neuropathol* 121:737–751 Available at: <http://www.rsb.info.nih.gov/ij/> [Accessed November 13, 2020].

Chidlow G, Wood JPM, Casson RJ (2017) Investigations into Hypoxia and Oxidative Stress at the Optic Nerve Head in a Rat Model of Glaucoma. *Front Neurosci* 11:478 Available at: <http://journal.frontiersin.org/article/10.3389/fnins.2017.00478/full> [Accessed October 24, 2019].

Chung CY, Koprach JB, Siddiqi H, Isacson O (2009) Dynamic changes in presynaptic and axonal transport proteins combined with striatal neuroinflammation precede dopaminergic neuronal loss in a rat model of AAV  $\alpha$ -synucleinopathy. *J Neurosci* 29:3365–3373 Available at: [www.jneurosci.org](http://www.jneurosci.org) [Accessed February 23, 2021].

Clarke LE, Liddelow SA, Chakraborty C, Münch AE, Heiman M, Barres BA (2018) Normal aging induces A1-like astrocyte reactivity. *Proc Natl Acad Sci U S A* 115:E1896–E1905 Available at: <http://www.ncbi.nlm.nih.gov/pubmed/29437957> [Accessed August 28, 2019].

Cooper ML, Pasini S, Lambert WS, D’Alessandro KB, Yao V, Risner ML, Calkins DJ (2020) Redistribution of metabolic resources through astrocyte networks mitigates neurodegenerative stress. *Texas Heal Sci Cent* 117:18810–18821.

Costantini LC, Barr LJ, Vogel JL, Henderson ST (2008) Hypometabolism as a therapeutic target in Alzheimer’s disease. In: *BMC Neuroscience*, pp S16. BioMed Central. Available at: [/pmc/articles/PMC2604900/](http://pmc/articles/PMC2604900/) [Accessed March 23, 2021].

Coughlin L, Morrison RS, Horner PJ, Inman DM (2015) Mitochondrial Morphology Differences and Mitophagy Deficit in Murine Glaucomatous Optic Nerve. *Invest Ophthalmol Vis Sci* 56:1437–1446 Available at: <http://iovs.arvojournals.org/Article.aspx?doi=10.1167/iovs.14-16126> [Accessed

September 11, 2019].

Crish SD, Dapper JD, MacNamee SE, Balaram P, Sidorova TN, Lambert WS, Calkins DJ (2013) Failure of axonal transport induces a spatially coincident increase in astrocyte BDNF prior to synapse loss in a central target. *Neuroscience* 229:55–70.

Dai C, Khaw PT, Yin ZQ, Li D, Raisman G, Li Y (2012) Structural basis of glaucoma: The fortified astrocytes of the optic nerve head are the target of raised intraocular pressure. *Glia* 60:13–28 Available at: <http://doi.wiley.com/10.1002/glia.21242> [Accessed January 26, 2020].

Dienel GA, Hertz L (2001) Glucose and lactate metabolism during brain activation. *J Neurosci Res* 66:824–838 Available at: <http://doi.wiley.com/10.1002/jnr.10079> [Accessed March 22, 2021].

Downs JC, Roberts MD, Burgoyne CF (2008) Mechanical environment of the optic nerve head in glaucoma. *Optom Vis Sci* 85:425–435 Available at: <http://www.ncbi.nlm.nih.gov/pubmed/18521012> [Accessed November 8, 2019].

El-Danaf RN, Huberman AD (2015) Characteristic patterns of dendritic remodeling in early-stage glaucoma: Evidence from genetically identified retinal ganglion cell types. *J Neurosci* 35:2329–2343 Available at: <https://www.jneurosci.org/content/35/6/2329> [Accessed March 23, 2021].

Flammer J, Orgül S, Costa VP, Orzalesi N, Kriegelstein GK, Serra LM, Renard JP, Stefánsson E (2002) The impact of ocular blood flow in glaucoma. *Prog Retin Eye Res* 21:359–393 Available at: <https://pubmed.ncbi.nlm.nih.gov/12150988/> [Accessed November 16, 2020].

Foltynie T (2019) Glycolysis as a therapeutic target for Parkinson’s disease. *Lancet Neurol* 18:1072–1074.

Fuchshofer R (2011) The pathogenic role of transforming growth factor- $\beta$ 2 in glaucomatous damage to the optic nerve head. *Exp Eye Res* 93:165–169.

- Gaude E, Schmidt C, Gammage PA, Dugourd A, Blacker T, Chew SP, Saez-Rodriguez J, O'Neill JS, Szabadkai G, Minczuk M, Frezza C (2018) NADH Shuttling Couples Cytosolic Reductive Carboxylation of Glutamine with Glycolysis in Cells with Mitochondrial Dysfunction. *Mol Cell* 69:581-593.e7 Available at: [/pmc/articles/PMC5823973/](https://pubmed.ncbi.nlm.nih.gov/30111111/) [Accessed March 26, 2021].
- Girard MJA, Beotra MR, Chin KS, Sandhu A, Clemo M, Nikita E, Kamal DS, Papadopoulos M, Mari JM, Aung T, Strouthidis NG (2016) In Vivo 3-Dimensional Strain Mapping of the Optic Nerve Head Following Intraocular Pressure Lowering by Trabeculectomy- *ClinicalKey*. *Ophthalmology* 123:1190–1200 Available at: <https://www.clinicalkey.com/#!/content/playContent/1-s2.0-S0161642016001706?returnurl=https%3A%2F%2Flinkinghub.elsevier.com%2Fretrieve%2Fpii%2FS0161642016001706%3Fshowall%3Dtrue&referrer=https%3A%2F%2Fwww.ncbi.nlm.nih.gov%2F> [Accessed October 17, 2019].
- Guo L, Tsatourian V, Luong V, Podolean AG, Jackson DA, Fitzke FW, Cordeiro MF (2005) En face optical coherence tomography: A new method to analyse structural changes of the optic nerve head in rat glaucoma. *Br J Ophthalmol* 89:1210–1216 Available at: <http://bj.o.bmj.com/> [Accessed February 22, 2021].
- Halestrap AP (2012) The monocarboxylate transporter family-Structure and functional characterization. *IUBMB Life* 64:1–9 Available at: <http://doi.wiley.com/10.1002/iub.573> [Accessed February 23, 2021].
- Harun-Or-Rashid M, Inman DM (2018) Reduced AMPK activation and increased HCAR activation drive anti-inflammatory response and neuroprotection in glaucoma. *J Neuroinflammation* 15:313 Available at: <https://jneuroinflammation.biomedcentral.com/articles/10.1186/s12974-018-1346-7> [Accessed March 11, 2019].
- Harun-Or-Rashid M, Pappenhagen N, Palmer PG, Smith MA, Gevorgyan V, Wilson GN, Crish SD, Inman

DM (2018) Structural and Functional Rescue of Chronic Metabolically Stressed Optic Nerves through Respiration. *J Neurosci* 38:5122–5139 Available at:

<http://www.ncbi.nlm.nih.gov/pubmed/29760184> [Accessed September 25, 2018].

Harun-Or-Rashid M, Pappenhagen N, Zubricky R, Coughlin L, Jassim AH, Inman DM (2020a) MCT2 Overexpression Rescues Metabolic Vulnerability and Protects Retinal Ganglion Cells in Two Models of Glaucoma. *bioRxiv:2020.02.14.950097* Available at:

<https://www.biorxiv.org/content/10.1101/2020.02.14.950097v1> [Accessed March 25, 2020].

Harun-Or-Rashid M, Pappenhagen N, Zubricky R, Coughlin L, Jassim AH, Inman DM (2020b) MCT2 Overexpression Rescues Metabolic Vulnerability and Protects Retinal Ganglion Cells in Two Models of Glaucoma. *bioRxiv:2020.02.14.950097* Available at:

<https://www.biorxiv.org/content/10.1101/2020.02.14.950097v1> [Accessed April 21, 2020].

Howell GR, Libby RT, Jakobs TC, Smith RS, Phalan FC, Barter JW, Barbay JM, Marchant JK, Mahesh N, Porciatti V, Whitmore A V, Masland RH, John SWM (2007) Axons of retinal ganglion cells are insulted in the optic nerve early in DBA/2J glaucoma. *J Cell Biol* 179:1523–1537 Available at:

<http://www.ncbi.nlm.nih.gov/pubmed/18158332> [Accessed September 23, 2019].

Huang C, Mattis P, Perrine K, Brown N, Dhawan V, Eidelberg D, Shore N (2008) Metabolic abnormalities associated with mild cognitive impairment in Parkinson disease HHS Public Access. *Neurology* 70:1470–1477.

Hui F, Tang J, Williams PA, McGuinness MB, Hadoux X, Casson RJ, Coote M, Trounce IA, Martin KR, Wijngaarden P, Crowston JG (2020) Improvement in inner retinal function in glaucoma with nicotinamide (vitamin B3) supplementation: A crossover randomized clinical trial. *Clin Experiment Ophthalmol* 48:903–914 Available at:

<https://onlinelibrary.wiley.com/doi/10.1111/ceo.13818> [Accessed March 23, 2021].

Iglesias J, Morales L, Barreto GE (2017) Metabolic and Inflammatory Adaptation of Reactive Astrocytes: Role of PPARs. *Mol Neurobiol* 54:2518–2538 Available at:

<http://link.springer.com/10.1007/s12035-016-9833-2> [Accessed September 25, 2019].

Jassim AH, Coughlin L, Harun-Or-Rashid M, Kang PT, Chen Y-R, Inman DM (2019) Higher Reliance on Glycolysis Limits Glycolytic Responsiveness in Degenerating Glaucomatous Optic Nerve. *Mol Neurobiol* 56:7097–7112 Available at: <http://link.springer.com/10.1007/s12035-019-1576-4>

[Accessed September 13, 2019].

Jassim AH, Fan Y, Pappenhagen N, Nsiah NY, Inman DM (2021) Oxidative Stress and Hypoxia Modifies Mitochondrial Homeostasis During Glaucoma. *Antioxid Redox Signal:ars.2020.8180* Available at:

<https://www.liebertpub.com/doi/10.1089/ars.2020.8180> [Accessed March 25, 2021].

Jassim AH, Inman DM (2019) Evidence of Hypoxic Glial Cells in a Model of Ocular Hypertension. *Investig Ophthalmology Vis Sci* 60:1 Available at:

<http://iovs.arvojournals.org/article.aspx?doi=10.1167/iovs.18-24977> [Accessed August 30, 2019].

Kaja S, Payne AJ, Patel KR, Naumchuk Y, Koulen P (2015) Differential subcellular Ca<sup>2+</sup> signaling in a highly specialized subpopulation of astrocytes. *Exp Neurol* 265:59–68 Available at:

<http://www.ncbi.nlm.nih.gov/pubmed/25542978> [Accessed March 10, 2020].

Laughton JD, Charnay Y, Belloir B, Pellerin L, Magistretti PJ, Bouras C (2000) Differential messenger RNA distribution of lactate dehydrogenase LDH-1 and LDH-5 isoforms in the rat brain. *Neuroscience* 96:619–625.

Lee JM, Calkins MJ, Chan K, Kan YW, Johnson JA (2003) Identification of the NF-E2-related factor-2-dependent genes conferring protection against oxidative stress in primary cortical astrocytes using oligonucleotide microarray analysis. *J Biol Chem* 278:12029–12038.

Libby RT, Anderson MG, Pang I-H, Robinson ZH, Savinova O V, Mihai Cosma I, Snow A, Wilson LA, Smith RS, Clark AF, John SWM (2005) Inherited glaucoma in DBA02J mice: Pertinent disease features for studying the neurodegeneration. Available at: <https://doi.org/10.1017/S0952523805225130> [Accessed October 23, 2018].

Liddelow SA et al. (2017) Neurotoxic reactive astrocytes are induced by activated microglia. *Nature* 541:481–487 Available at: <http://www.nature.com/articles/nature21029> [Accessed October 18, 2019].

Lum JJ, Bui T, Gruber M, Gordan JD, DeBerardinis RJ, Covello KL, Simon MC, Thompson CB (2007) The transcription factor HIF-1 plays a critical role in the growth factor-dependent regulation of both aerobic and anaerobic glycolysis. *Genes Dev* 21:1037–1049 Available at: </pmc/articles/PMC1855230/> [Accessed April 19, 2021].

Maddineni P, Kasetti RB, Patel PD, Millar JC, Kiehlbauch C, Clark AF, Zode GS (2020) CNS axonal degeneration and transport deficits at the optic nerve head precede structural and functional loss of retinal ganglion cells in a mouse model of glaucoma. *Mol Neurodegener* 15:1–20 Available at: <https://link.springer.com/articles/10.1186/s13024-020-00400-9> [Accessed October 18, 2020].

Malone P, Miao H, Parker A, Juarez S, Hernandez MR (2007) Pressure induces loss of gap junction communication and redistribution of connexin 43 in astrocytes. *Glia* 55:1085–1098 Available at: <http://doi.wiley.com/10.1002/glia.20527> [Accessed October 31, 2019].

Minckler DS (1980) The Organization of Nerve Fiber Bundles in the Primate Optic Nerve Head. *Arch Ophthalmol* 98:1630–1636 Available at: <https://jamanetwork.com/journals/jamaophthalmology/fullarticle/633531> [Accessed November 10, 2020].

- Mookerjee SA, Goncalves RLS, Gerencser AA, Nicholls DG, Brand MD (2015) The contributions of respiration and glycolysis to extracellular acid production. *Biochim Biophys Acta - Bioenerg* 1847:171–181.
- Morgello S, Uson RR, Schwartz EJ, Haber RS (1995) The human blood-brain barrier glucose transporter (GLUT1) is a glucose transporter of gray matter astrocytes. *Glia* 14:43–54 Available at: <https://pubmed.ncbi.nlm.nih.gov/7615345/> [Accessed February 18, 2021].
- Morita M, Ikeshima-Kataoka H, Kreft M, Vardjan N, Zorec R, Noda M (2019) Metabolic plasticity of astrocytes and aging of the brain. *Int J Mol Sci* 20:941 Available at: [www.mdpi.com/journal/ijms](http://www.mdpi.com/journal/ijms) [Accessed March 10, 2021].
- Munemasa Y, Kitaoka Y (2012) Molecular mechanisms of retinal ganglion cell degeneration in glaucoma and future prospects for cell body and axonal protection. *Front Cell Neurosci* 6:60 Available at: [www.frontiersin.org](http://www.frontiersin.org) [Accessed February 22, 2021].
- Muraleedharan R, Gawali M V., Tiwari D, Sukumaran A, Oatman N, Anderson J, Nardini D, Bhuiyan MAN, Tkáč I, Ward AL, Kundu M, Waclaw R, Chow LM, Gross C, Rao R, Schirmeier S, Dasgupta B (2020) AMPK-Regulated Astrocytic Lactate Shuttle Plays a Non-Cell-Autonomous Role in Neuronal Survival. *Cell Rep* 32 Available at: <https://doi.org/10.1016/j.celrep.2020.108092> [Accessed February 24, 2021].
- Nagao A, Kobayashi M, Koyasu S, Chow CCT, Harada H (2019) HIF-1-dependent reprogramming of glucose metabolic pathway of cancer cells and its therapeutic significance. *Int J Mol Sci* 20 Available at: [/pmc/articles/PMC6359724/](https://pubmed.ncbi.nlm.nih.gov/35459724/) [Accessed April 19, 2021].
- O'Brien J, Kla KM, Hopkins IB, Malecki EA, McKenna MC (2007) Kinetic Parameters and Lactate Dehydrogenase Isozyme Activities Support Possible Lactate Utilization by Neurons. *Neurochem Res*

32:597–607 Available at: <http://link.springer.com/10.1007/s11064-006-9132-9> [Accessed November 6, 2019].

Pellerin L, Pellegrini G, Bittar PG, Charnay Y, Bouras C, Martin J-L, Stella N, Magistretti PJ (1998) Evidence Supporting the Existence of an Activity-Dependent Astrocyte-Neuron Lactate Shuttle. *Dev Neurosci* 20:291–299 Available at: <http://www.ncbi.nlm.nih.gov/pubmed/9778565> [Accessed September 17, 2019].

Plaitakis A, Kalef-Ezra E, Kotzamani D, Zaganas I, Spanaki C (2017) The glutamate dehydrogenase pathway and its roles in cell and tissue biology in health and disease. *Biology (Basel)* 6:11 Available at: [/pmc/articles/PMC5372004/](https://pubmed.ncbi.nlm.nih.gov/32012756/) [Accessed March 12, 2021].

Prokai L, Zaman K, Nguyen V, Prokai-Tatrai K (2020) 17 $\beta$ -estradiol delivered in eye drops: Evidence of impact on protein networks and associated biological processes in the rat retina through quantitative proteomics. *Pharmaceutics* 12 Available at: <https://pubmed.ncbi.nlm.nih.gov/32012756/> [Accessed March 22, 2021].

Quigley HA, Addicks EM, Green WR, Maumenee AE (1981) Optic nerve damage in human glaucoma: I. The Site of Injury and Susceptibility to Damage. *Arch Ophthalmol* 99:635–649 Available at: <https://pubmed.ncbi.nlm.nih.gov/6164357/> [Accessed November 13, 2020].

Quigley HA, Green WR (1978) The Histology of Human Glaucoma Cupping and Optic Nerve Damage: Clinicopathologic Correlation in 21 Eyes. *Ophthalmology* 127:S45–S69.

Rahman MH, Suk K (2020) Mitochondrial Dynamics and Bioenergetic Alteration During Inflammatory Activation of Astrocytes. *Front Aging Neurosci* 12:459 Available at: <https://www.frontiersin.org/articles/10.3389/fnagi.2020.614410/full> [Accessed March 22, 2021].

Reitman ZJ, Yan H (2010) Isocitrate Dehydrogenase 1 and 2 Mutations in Cancer: Alterations at a

Crossroads of Cellular Metabolism. *JNCI J Natl Cancer Inst* 102:932–941 Available at:  
<https://academic.oup.com/jnci/article-lookup/doi/10.1093/jnci/djq187> [Accessed March 12, 2021].

Rogers R, Dharsee M, Ackloo S, Flanagan JG (2012a) Proteomics Analyses of Activated Human Optic Nerve Head Lamina Cribrosa Cells following Biomechanical Strain. *Investig Ophthalmology Vis Sci* 53:3806 Available at: <http://iovs.arvojournals.org/article.aspx?doi=10.1167/iovs.11-8480> [Accessed January 10, 2020].

Rogers RS, Dharsee M, Ackloo S, Sivak JM, Flanagan JG (2012b) Proteomics analyses of human optic nerve head astrocytes following biomechanical strain. *Mol Cell Proteomics* 11:M111.012302 Available at: <http://www.ncbi.nlm.nih.gov/pubmed/22126795> [Accessed February 20, 2020].

Rose J, Brian C, Pappa A, Panayiotidis MI, Franco R (2020) Mitochondrial Metabolism in Astrocytes Regulates Brain Bioenergetics, Neurotransmission and Redox Balance. *Front Neurosci* 14:1155 Available at: [www.frontiersin.org](http://www.frontiersin.org) [Accessed March 18, 2021].

Saab AS et al. (2016) Oligodendroglial NMDA Receptors Regulate Glucose Import and Axonal Energy Metabolism. *Neuron* 91:119–132 Available at:  
<https://www.sciencedirect.com/science/article/pii/S0896627316301763> [Accessed March 10, 2020].

Saleh M, Nagaraju M, Porciatti V (2007) Longitudinal evaluation of retinal ganglion cell function and IOP in the DBA/2J mouse model of glaucoma. *Investig Ophthalmol Vis Sci* 48:4564–4572 Available at:  
<http://rsb.info.nih.gov/nih-image/>; [Accessed February 17, 2021].

Sheng WS, Hu S, Feng A, Rock RB (2013) Reactive oxygen species from human astrocytes induced functional impairment and oxidative damage. *Neurochem Res* 38:2148–2159 Available at:

<https://link.springer.com/article/10.1007/s11064-013-1123-z> [Accessed March 22, 2021].

Steele ML, Robinson SR (2012) Reactive astrocytes give neurons less support: implications for Alzheimer's disease. *Neurobiol Aging* 33:423.e1-423.e13 Available at: <https://www.sciencedirect.com/science/article/abs/pii/S0197458010003982> [Accessed September 18, 2019].

Sun D, Lye-Barthel M, Masland RH, Jakobs TC (2010) Structural remodeling of fibrous astrocytes after axonal injury. *J Neurosci* 30:14008–14019 Available at: <http://www.ncbi.nlm.nih.gov/pubmed/20962222> [Accessed September 19, 2018].

Supplie LM, Düking T, Campbell G, Diaz F, Moraes CT, Götz M, Hamprecht B, Boretius S, Mahad D, Nave K-A (2017) Respiration-Deficient Astrocytes Survive As Glycolytic Cells In Vivo. *J Neurosci* 37:4231–4242 Available at: <http://www.ncbi.nlm.nih.gov/pubmed/28314814> [Accessed October 23, 2019].

Tang BL (2020) Glucose, glycolysis, and neurodegenerative diseases. *J Cell Physiol* 235:7653–7662 Available at: <https://onlinelibrary.wiley.com/doi/10.1002/jcp.29682> [Accessed March 23, 2021].

Tanner LB, Goglia AG, Wei MH, Sehgal T, Parsons LR, Park JO, White E, Toettcher JE, Rabinowitz JD (2018) Four Key Steps Control Glycolytic Flux in Mammalian Cells. *Cell Syst* 7:49-62.e8 Available at: <https://www.sciencedirect.com/science/article/pii/S2405471218302436> [Accessed October 3, 2019].

Tezel G, Wax MB (2004) Hypoxia-inducible factor 1 $\alpha$  in the glaucomatous retina and optic nerve head. *Arch Ophthalmol* 122:1348–1356 Available at: <https://jamanetwork.com/> [Accessed March 23, 2021].

Turner DA, Adamson DC (2011) Neuronal-astrocyte metabolic interactions: Understanding the transition into abnormal astrocytoma metabolism. *J Neuropathol Exp Neurol* 70:167–176 Available at:

/pmc/articles/PMC3045672/ [Accessed March 12, 2021].

Vicente-Gutiérrez C, Jiménez-Blasco D, Quintana-Cabrera R (2021) Intertwined ROS and Metabolic Signaling at the Neuron-Astrocyte Interface. *Neurochem Res* 46:23–33.

Vohra R, Tsai JC, Kolko M (2013) The Role of Inflammation in the Pathogenesis of Glaucoma. *Surv Ophthalmol* 58:311–320 Available at:  
<https://www.sciencedirect.com/science/article/pii/S0039625712001907> [Accessed September 25, 2019].

Volkenhoff A, Weiler A, Letzel M, Stehling M, Klämbt C, Schirmeier S (2015) Glial Glycolysis Is Essential for Neuronal Survival in *Drosophila*. *Cell Metab* 22:437–447 Available at:  
<https://www.sciencedirect.com/science/article/pii/S1550413115003356?via%3Dihub> [Accessed September 25, 2019].

Weinreb RN, Aung T, Medeiros FA (2014) The pathophysiology and treatment of glaucoma: A review. *JAMA - J Am Med Assoc* 311:1901–1911 Available at: <https://jamanetwork.com/> [Accessed October 16, 2020].

Williams PA, Harder JM, Foxworth NE, Cochran KE, Philip VM, Porciatti V, Smithies O, John SWM (2017) Vitamin B3 modulates mitochondrial vulnerability and prevents glaucoma in aged mice. *Science* (80- ) 355:756–760.

Wilson GN, Smith MA, Inman DM, Dengler-Crish CM, Crish SD (2016) Early Cytoskeletal Protein Modifications Precede Overt Structural Degeneration in the DBA/2J Mouse Model of Glaucoma. *Front Neurosci* 10:494 Available at:  
<http://journal.frontiersin.org/article/10.3389/fnins.2016.00494/full> [Accessed September 26, 2018].

Wordinger RJ, Sharma T, Clark AF (2014) The role of TGF- $\beta$ 2 and bone morphogenetic proteins in the trabecular meshwork and glaucoma. *J Ocul Pharmacol Ther* 30:154–162 Available at: <https://www.liebertpub.com/doi/abs/10.1089/jop.2013.0220> [Accessed March 25, 2021].

Wu M, Neilson A, Swift AL, Moran R, Tamagnine J, Parslow D, Armistead S, Lemire K, Orrell J, Teich J, Chomicz S, Ferrick DA (2007) Multiparameter metabolic analysis reveals a close link between attenuated mitochondrial bioenergetic function and enhanced glycolysis dependency in human tumor cells. *Am J Physiol - Cell Physiol* 292:125–136 Available at: [www.ajpcell.org](http://www.ajpcell.org) [Accessed February 15, 2021].

Xie H, Cui Y, Hou S, Wang J, Miao J, Deng F, Feng J (2017) Evaluation of Connexin 43 Redistribution and Endocytosis in Astrocytes Subjected to Ischemia/Reperfusion or Oxygen-Glucose Deprivation and Reoxygenation. *Biomed Res Int* 2017.

Zamanian JL, Xu L, Foo LC, Nouri N, Zhou L, Giffard RG, Barres BA (2012) Genomic Analysis of Reactive Astrogliosis. *Neurobiol Dis* 32:6391–6410 Available at: <http://www.ncbi.nlm.nih.gov/geo/query/acc.cgi?acc=GSE35338> [Accessed March 22, 2021].

Zhang L, Albon J, Jones H, Gouget CLM, Ethier CR, Goh JCH, Girard MJA (2015) Collagen microstructural factors influencing optic nerve head biomechanics. *Invest Ophthalmol Vis Sci* 56:2031–2042 Available at: [www.iovs.org](http://www.iovs.org) [Accessed March 25, 2021].

Zode GS, Clark AF, Wordinger RJ (2009) Bone morphogenetic protein 4 inhibits TGF- $\beta$ 2 stimulation of extracellular matrix proteins in optic nerve head cells: Role of gremlin in ECM modulation. *Glia* 57:755–766 Available at: <http://doi.wiley.com/10.1002/glia.20803> [Accessed March 25, 2021].

Zode GS, Sethi A, Brun-Zinkernagel AM, Chang IF, Clark AF, Wordinger RJ (2011) Transforming growth factor- $\beta$ 2 increases extracellular matrix proteins in optic nerve head cells via activation of the smad

signaling pathway. Mol Vis 17:1745–1758 Available at: <http://www.molvis.org/molvis/v17/a192>  
[Accessed March 25, 2021].